Mouse Fc and Fab IgG N-glycosylation

Vuković, Nikolina

Master's thesis / Diplomski rad

2021

Degree Grantor / Ustanova koja je dodijelila akademski / stručni stupanj: **University of Zagreb, Faculty of Science / Sveučilište u Zagrebu, Prirodoslovno-matematički fakultet**

Permanent link / Trajna poveznica: https://urn.nsk.hr/urn:nbn:hr:217:427228

Rights / Prava: In copyright/Zaštićeno autorskim pravom.

Download date / Datum preuzimanja: **2025-02-02**

University of Zagreb

Faculty of Science

Department of Biology

Nikolina Vuković

Mouse Fc and Fab IgG *N*-glycosylation

Master thesis

Zagreb, 2021.

« This Master thesis was performed in Genos Ltd. under mentorship of dr. sc. Marija Pezer. The manuscript was submitted for evaluation to the Department of Biology, Faculty of Science, University of Zagreb in order to obtain the title of Master of Experimental Biology (mag. biol. exp.) »

Mouse Fc and Fab IgG *N*-glycosylation

Nikolina Vuković

Roosveltov trg 6, 10 000 Zagreb, Croatia

N-glycans are complex oligosaccharides bound to the nitrogen atom of asparagine. Immunoglobulin G (IgG) molecule contains two *N*-glycans attached to the fragment crystallizable (Fc) region, but only a minority of IgG molecules contain antigen binding fragment (Fab) *N*-glycans. Both Fab and Fc *N*-glycans influence the molecule's function in the immune response, a phenomenon often explored through mouse models. The aim of this study was to establish an analytical method for comparative *N*-glycosylation analysis of mouse Fc and Fab IgG fragments based on the method used for human IgG. IgG was isolated by affinity chromatography from serum of CBAT6T6 mice. The optimized protocol included a 20h-digestion on Fc beads in reducing conditions and fragments separation. Each IgG portion was deglycosylated and the released *N*-glycans were fluorescently labelled and analysed by capillary gel-electrophoresis with laser-induced fluorescence on an DNA sequencer. Collected data were processed in the Empower program. A total of 35 *N*-glycan peaks were defined and 16 of them annotated. The initially implemented method for the analysis of mouse Fab and Fc IgG *N*-glycans is judged functional. The comparison of proportion height percentages (PHP%) showed differences in the Fab and Fc glycoprofile similar to those observed for human IgG.

TEMELJNA DOKUMENTACIJSKA KARTICA

N-glikozilacija fragmenata Fc i Fab mišjeg imunoglobulina G

Nikolina Vuković

Roosveltov trg 6, 10 000 Zagreb, Hrvatska

N-glikani su kompleksni oligosaharidi vezani na dušikov atom asparagine. Imunoglobulin G (IgG) sadrži dva *N*-glikana vezana na kristalizirajućem fragmentu (Fc). Manji udio molekula IgG ima vezane *N*-glikane na antitijelo vezujućem fragment (Fab). Fab i Fc *N*-glikani utječu na funkciju molekule IgG u imunološkom odgovoru, što se često istražuje na mišjim modelima. Cilj ovog diplomskog rada je bio uspostaviti analitičku metodu za usporednu analizu *N*-glikozilacije Fc i Fab fragmenta mišjeg imunoglobulina G na temelju metode koja se koristi za analizu glikoma ljudskog IgG-a. IgG je izoliran afinitetnom kromatografijom iz seruma miševa soja CBAT6T6. Optimirani protokol uključuje dvadesetsatnu razgradnju na kuglicama specifičnim za Fc fragment u reducirajućim uvjetima. Nakon razgradnje na Fab i Fc fragment, uzorci su deglikozilirani. Oslobođeni *N*-glikani su fluorescentno obilježeni i analizirani kapilarnom gel-elektroforezom s laserom induciranom fluorescencijom u DNA sekvenceru. Prikupljeni podaci su obrađeni u programu Empower. Ukupno je određeno 35 *N*-glikanskih pikova, od kojih je za njih 16 otprije poznat *N*-glikanski sastav. Inicijalno upotrijebljena metoda za analizu *N*-glikana Fab i Fc fragmenta mišjeg IgG-a procijenjena je učinkovitom. Usporedba postotaka ukupne visine (PHP%) pojedinih pikova pokazala je razlike u glikanskom profilu Fc i Fab fragmenata nalik onima uočenim kod ljudskog IgG-a.

Abbreviations

ADCC - antibody-dependent cell-mediated cytotoxicity

APCs - antigen presenting cells

Asn – Asparagine

CDC - complement-dependent cytotoxicity

CDRs – complementary determining regions

D_H - diversity heavy chain

Dol-PP – dolichol pyrophosphate

Fab – fragment antigen-binding

Fc – fragment crystallizable

FcR – Fc receptor

Fuc – fucose

GlcNAc – *N*-acetylglucosamine

GalNAc – *N*-acetylgalactosamine

HC – heavy chain

IL-4 – interleukin 4

LC – light chain

Man – mannose

NHEJ – non homologous end joining

Neu5Ac – *N*-acetylneuraminic acid

Neu5Gc - *N*-glycolylneuraminic acid

OST – oligosaccharyl transferase

Pro – Proline

RAGs – recombination activating genes

RSS - recombination signal sequence

RGYW - purine G/pyrimidine A motif

Sia – sialic acid

Ser – Serine

SHM - somatic hyper mutation

Thr – Threonine

Table of Contents

1. Introduction

1.1. Protein glycosylation

After the translation in cell cytoplasm, every protein goes through various modifications which will influence its final function. Glycosylation is one of the most significant posttranslational modifications that occurs in the inner part of endoplasmic reticulum (ER) and in Golgi apparatus. Carbohydrates covalently bind to nitrogen atom in the asparagine residue (*N*-linkage) or oxygen atom in the serine or threonine residue (*O*-linkage) (Figure 1.). Such modified proteins are then transported to certain cell compartments. Most of the glycoproteins are part of the cell membrane where they are involved in intercellular communication or adhesion. Some of them are take part in posttranslational protein formation in the ER, where they help other polypeptides adopt the right structure and direct them to intended compartments. Also, many glycoproteins are secreted outside of the cell, just like immunoglobulins are secreted from mature B cells (plasma cells) in blood serum (Cooper and Hausman, 2010; Stryer, 2013).
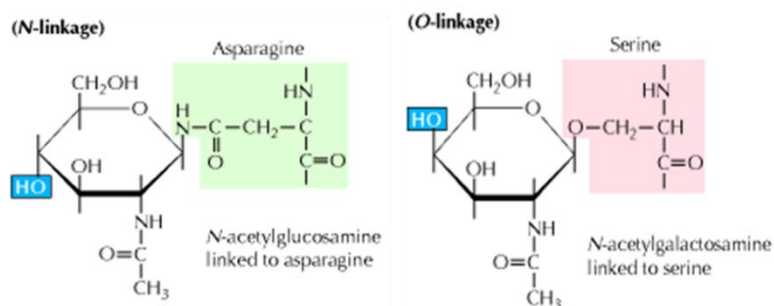
Figure 1. N- and *O*-linked glycosidic bond between glycans and amino acid residues (Cooper and Hausman, 2010).

1.1.1. *N*-glycans

In the glycosylation process, proteins covalently bind single carbohydrates (monosaccharides) or carbohydrate chains (oligosaccharides and polysaccharides). Glycans are complex carbohydrate chains composed of single monosaccharides. Except the fact they are structure molecules, they also have an important role in maintenance of normal biological functions in the organism (Varki *et al*., 2017). *N*-glycans in eukaryotes specifically bind to asparagine (Asn) in polypeptide sequence Asn-X-Ser/Thr where "X" is any amino acid except

Pro. The *N*-glycosidic bond is established between Asn and *N*-acetylglucosamine in the glycan. Nevertheless, not all Asn residues in motif sequence are glycosylated.

Eukaryotic *N*-glycans have an identical core structure built from three mannose (Man) and two *N*-acetylglucosamine molecules (GlcNAc). Furthermore, additional sugar residues are attached on $Man_3GlcNAc_2$-Asn. Most common ones are: fucose (Fuc), galactose (Gal), *N*-acetylgalactosamine (GalNAc), *N*-acetylglucosamine and sialic acid (Sia). Considering core structure and connected residues, there are three types of *N*-glycans: oligomannose, complex and hybrid types (Stryer 2013., Varki *et al*., 2017). Oligomannose types have two to nine mannoses in contrast to complex type *N*-glycans. They have a heterogeneous highly branched structure with one or more GlcNAc, Gal or Sia on each antenna. Hybrid type glycans have one antenna compounded from mannose residues, and one complex type-like branch with different residues on it (Figure 2.). Glycans with one branch are called monoatennary and the ones with two branches are called biantennary glycans (Gornik and Lauc, 2008; Bieberich, 2014).
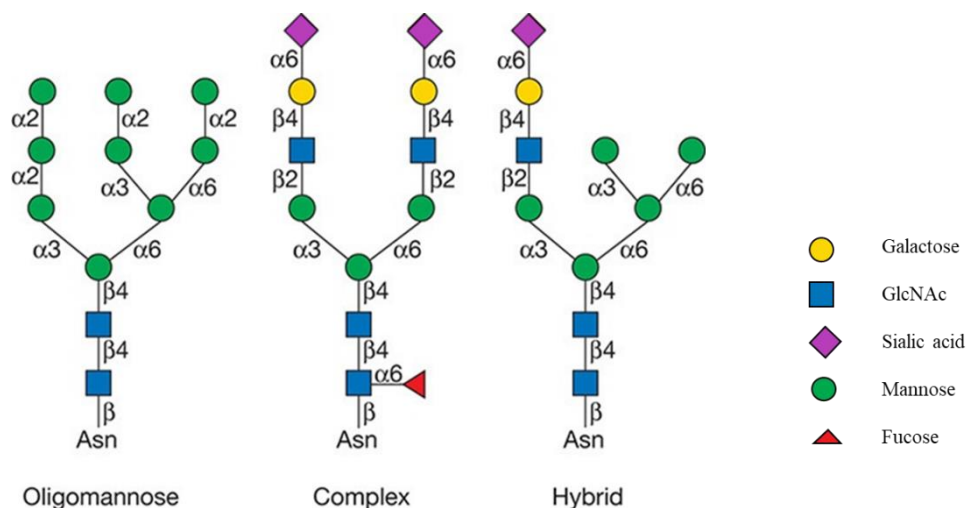
Figure 2. The monosaccharide residues are color-coded according to the recommendation by the Consortium for Functional Glycomics *(*Symbol and Text Nomenclature for Representation of Glycan Structure Nomenclature Committee Consortium for Functional Glycomics*, 2012).*

1.1.2. Biosynthesis of *N*-glycans in eukaryotes

After the translation on ribosome, the polypeptide chain that is meant to be glycosylated is transferred and bound to the cytoplasmic side of ER (endoplasmic reticulum). Then the whole molecule is transferred through the membrane into the ER lumen. Unlike the O-glycosylation, which takes place exclusively in the Golgi apparatus, *N*-glycosylation starts in the ER and

finishes in the Golgi apparatus. Oligosaccharide, which will bound to Asn in Asn-X-Ser/Thr sequon, is placed on the inner side of the ER membrane. After this, synthesized sugar core is attached to dolichol pyrophosphate (Dol-PP) via pyro domain. Dol-PP is a lipid molecule compounded from up to 20 isoprene units which carries oligosaccharide until the reaction of forming glycoprotein. The oligosaccharide precursor has a $Glc_3Man_9GlcNAc_2$ structure and is formed in reactions catalyzed by enzymes placed on both sides (luminal and cytoplasmic) of the ER (Stryer 2013., Bieberich, 2014). Different ER membrane associated glycosyltransferase types add residues on Dol-PP. First *N*-acetylglucosaminyltransferase attaches two GlcNAc molecules in β1-*N* and β1-4 linkage. Then, mannosyltransferases are catalyzing four linkages: β-1,4 (mannose is binding to second GlcNAc), α-1,3 and two α-1,6 bonds (two mannose molecules on branching points in oligosaccharide). Two more mannoses are attached via α-1,2 linkage on one branch with previously bound mannose (α-1,6). Additionally, oligosaccharide precursor is transported through the ER membrane in lumen where more residues will be attached. Via α-1,2 linkage, two mannose elongates are added on the first antennae and one elongate is added on two separated branches. Glucosyltransferases bind two glucose residues in α-1,3 and one in α-1,2 linkage, all three attaching to the first mannose antennae. The activated sugar molecules, which are produced on the inner and outer ER membrane, are important for successful binding reactions. They are in the form of UDP-GlcNAc (uridine diphosphate *N*-acetyglycosamine), GDP-mannose (guanosine diphosphate mannose), and UDP-glucose (uridine diphosphate glucose) (Bieberich, 2014).

The transfer of precursor oligosaccharide on a nascent polypeptide chain is controlled by the enzyme OST (oligosaccharyl transferase) that is highly specific for Asn residues only in Asn-X-Ser and Asn-X-Thr sequence. OST attaches the $Glc_3Man_9GlcNAc_2$ from the Dol-PP on Asn in polypeptide chain in the ER lumen. Regardless of the enzymes specificity, not all Asn-X-Ser/Thr sequences are glycosylated. Because of the fast protein folding in the ER, the target Asn can stay inaccessible to the OST. (Bieberich, 2014., Loodish *et al.,* 2000).

The $Glc_3Man_9GlcNAc_2$ is cleaved via glucosidase-dependent and independent pathway. Since there is a lack of information on glucosidase-independent pathway, it still needs to be studied how an endomannosidase enzyme cleaves off a Glc1-3Man1 molecule in Golgi apparatus.

On the other side, glucosidase-dependent pathway is known for a chaperon activity in the protein folding after enzymes glucosidase I and II cleave terminal glucose residues in ER. The chaperon role is to recognize and bind misfolded proteins in order to stabilize them. In addition, the chaperon role is also for interfering in the refolding process until the protein folds in the

appropriate conformation. First, glucosidase enzymes I and II cleave the two glucose molecules from the $Glc_3Man_9GlcNAc_2$ oligosaccharide residue. The $GlcMan_9GlcNAc_2$ residue with a protein sequence binds to chaperones calreticulin or calnexin. They can specifically bind to monoglucosylated *N*-glycoproteins ($GlcMan_9GlcNAc_2$). If the glycoprotein does not fold properly, it is degraded by the ERAD (ER-assisted degradation system) or transferred to Golgi. After that, the glycoprotein is transferred to lysosomes where later is proteolytically digested. When the $GlcMan_9GlcNAc_2$ glycoprotein is bound to chaperons, at the same time the peptide part starts unfolding and the glucosidase II removes the inner glucose to form the $Man_9GlcNAc_2$. In order to prevent a degradation of the protein part which still has not folded properly, the glycoprotein glucosyltransferase temporary reglucosylate the current *N*-glycan $Man_9GlcNAc_2$ with the activated sugar UDP-glucose. The enzyme glucosidase II once again cleaves the lastly added Glc, and the glycoprotein structure goes through reactions of refolding and reglucosylation until the peptide part gets in an adequate conformation. When this process is finished, the $Man_9GlcNAc_2$ undergoes cleaving reactions in which the mannosidase I from the ER will enable the final $Man_5GlcNAc_2$. After that, the UDP-GlcNAc transferase I binds one GlcNAc molecule to the first branch which finish with a mannose. The final $GlcNAcMan_5GlcNAc_2$ is then elongated by adding more sugar residues: GlcNAc, Sia, Gal and Fuc for hybrid *N*-glycans and GlcNAc, Sia, and Fuc for complex *N*-glycans (Stryer 2013., Bieberich, 2014).

1.2.   Immunoglobulin G

Immunoglobulin (IgG) is one of the most prevalent proteins in serum. In healthy individuals, it is the most abundant antibody with serum concentrations from 7 to 18 mg/mL. It has an prominent role in immune responses such as antibody-dependent cell-mediated cytotoxicity (ADCC), antigen neutralization, complement activation, complement-dependent cytotoxicity (CDC), target opsonization for phagocytosis, and hypersensitivity reactions (Gudelj *et al*, 2018).

Out of the five antibody isotypes (IgA, IgD, IgE, IgG, IgM), only IgA and IgG are divided into subclasses. There are four subtypes of murine IgG (IgG1, IgG2a/c, IgG2b and IgG3). Although the mouse and human IgG have a similar amino acid structure, they differ in the functional potency to bind to receptors (FcRs, fragment crystallizable receptors), activate complement, half-life, and placental transport. Because of its long half-life and important role in various immune pathways, IgG is the mainly antibody type used in monoclonal therapeutics (Vidarsson *et al.*, 2014; Lu *et al.*, 2017).

Mouse (lat. *Mus musculus*) is the most commonly used animal model in immunological translational studies. It has an immune system similar to human, and can be relatively easily observed in laboratory conditions (Reiding *et al.*, 2016a). However, mice differ from humans in some properties, such as functions of IgG subclasses and antibody levels. Some mouse strains (CB57BL/6, CB57BL/10, SJL, and NOD) do not express usual IgG2b but IgG2c. Neither of these variants are direct homologues of the human IgG2. In the process of class switching regulated by interleukins, IL-4 (interleukin 4) in mouse induces IgG1 and IgE while in human IgG4 and IgE. (Mestas and Hughes, 2004). So far, the humanized mice models in biomedical research seem to give answers to some questions. However, when it comes to IgG *N*-glycosylation, the question remains to which extent the glycosylation-induced changes in IgG effector functions are translatable between mice and human. Glycosylation of IgG makes the translation of studies performed on mice to human setting quite challenging. Previous research showed structural distinctions among subclasses and significant variations of glycosylation pattern among different mouse strains. Also, some of the IgG glycosylation features present in mice are absent on human IgG, such as α-Gal epitope and *N*-glycolylneuraminic acid (Zaytseva *et al.*, 2018). This adds another layer of complexity to using mouse models for studying human IgG glycosylation and its immune context.

1.2.1. Immunoglobulin structure

All immunoglobulins or antibodies are made of two heavy chains (HCs) and two light chains (LCs) that are mutually connected with up to 12 disulfide bonds. HCs are connected by a variable number of disulfide bonds in the hinge region. LCs are connected to HCs by a disulfide bond between cysteine residues (Liu and May, 2012). Together, the two same HC-LC dimers make the structure of an antibody. Among Ig subclasses, different genes are coding mRNA for HCs amino acidic sequence. Each subclass has its specific heavy chain type: α (IgA), δ (IgD), ε (IgE), γ (IgG), μ (IgM). Main differences between them are in size and carbohydrate content. On the other side, there are two main subclasses of light chains: κ (lat. *kappa*) and γ (lat. *lambda*). Although they are chemically similar, they differ in amino acid content in one constant region. All Ig subclasses can either have a κ or γ light chain, but never the both. A specific combination of heavy and light chains together in immunoglobulin makes them differ in structure and function.

Each chain in immunoglobulin structure has three-dimensional folded structures - one NH2-terminal variable domain (V) and one or more repeating COOH-terminal constant

domains (C). The C and V domains are built from around 110 to 130 amino acids. HCs have three or four C domains and one V domain. HCs that are built from three C domains have between the first and second domain a large hinge region. LCs are made of one V and one C domain (Figure 3.). Both C and V domains are specific for proteins from the immunoglobulin superfamily (IgSF) (Schroeder and Cavacini, 2010). The IgG contains 12 Ig domains out of which all have the same folding structure made from β-antiparallel strands. Those strands form two β-sheets connected by disulfide bonds between conserved cysteine residues (Stryer, 2013).

The chains are called heavy and light because of the notable mass difference. Total mass of an antibody is approximately 150 kDa, from which LCs together weight 50 kDa, and HCs with hinge region weigh 100-110 kDa. There is a variation in mass through Ig subclasses depending on HC type, molecules that can bind externally between β-strands on the loops surface, and carbohydrate content (Schroeder and Cavacini, 2010).

On one hand, studies based on amino acid sequence of IgG chains showed that carboxyl terminal L_C and H_C regions are very similar. On the other hand, amino terminal L_V and H_V regions showed significant difference in three segments made of 7-12 amino acids on each chain. These segments are called complementarity-determining regions (CDRs) or hypervariable loops. Such variety is crucial for producing numerous antibodies with the ability of recognizing different antigens (Stryer, 2013).

Antigens are molecules that cause the activation of the adaptive immune system. Usually, they imply surface structures on viruses, bacteria, foreign cells or native cells (autoimmune diseases). They are divided by their origin and final immune response. Immunogens are antigens which activate T cells and antigen presenting cells (APCs) in order to initiate B cells on clonal selection and later, the production of antibodies. Those antibodies are B cell receptors up until the immunogen mediated activation, after which they are secreted from plasma cells (matured B cells) with the purpose of marking the same immunogen and neutralizing it. This reaction is a typical adaptive immune response. Antigens which do not cause the production of antibodies are diminished with macrophages or T cells as a part of the innate immune response.

An antibody and antigen associate through a complementary recognition and non-covalent interactions between the epitope and paratope. The epitope is a binding site on an antigen and the paratope is a binding site on an antibody compounded from the CDRs (Sela-Culang *et al.*, 2013).
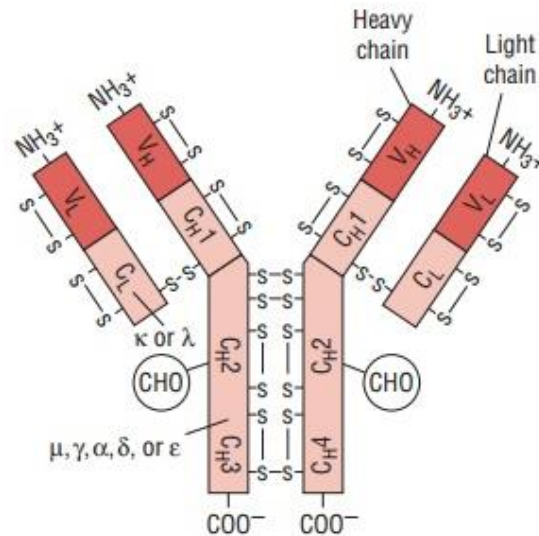
Figure 3. Immunoglobulin structure with heavy chain and light chain domains
(http://www.brainkart.com/article/Structure-of-Immunoglobulins_17908/).

1.2.2. Fab and Fc

The antibody structure for all five subclasses is also defined by the antigen-binding fragment (Fab) part and the fragment crystallizable (Fc) part. Fab includes complete LCs, V_H and C_H1 domains from both HCs. The rest of the constant regions of heavy chains (C_H2, C_H3 and C_H4) are conforming to the Fc part. Together, they are giving "T" or "Y" shape to an antibody. There is a flexible hinge region between fragments. The length and flexibility of this part vary among antibody classes and subclasses. It also affects directly possible conformations of the Fab to the Fc part (Vidarsson *et al*, 2014).

The Fc part got the name from its tendency to crystallize. There are five isotypes of the Fc among the antibody classes. They are structurally unique, but can change during the immune response to initiate specific reactions via binding on various fragment crystallizable receptors (FcRs), fragment crystallizable receptor neonatal (FcRn*)*, and complement component C1q (Vidarsson *et al.*, 2014; Lu *et al.*, 2017). The Fc fragment of the IgG binds to Fcγ receptors. They can only bind antibodies with γ HCs in the Fc part. Changes in the Fc region affect the terminal outcome of an antigen-antibody interaction, as well as the antibody affinity and kinetics of binding to an antigen (Schroeder and Cavacini, 2010).

Within the Fc region is a highly conserved glycosylation site on the asparagine 297 which is placed on the second Ig domain of HC (CH_2) (Figure 4.). The *N*-glycans attached to Asn-297 influence IgG function. They are a complex biantennary type glycans made from bisecting (GlcNAc), mannose, core fucose (Fuc), galactose (Gal), and terminal *N*-acetylneuraminic acid

(Neu5Ac/sialic acid) residues. The difference in residues ratio will directly promote pro- or anti-inflammatory immune activity (Cobb, 2019).

N-glycans on the Fc part and their influence on IgG function is far more researched than the ones on the Fab part. This lack of information is specially related to the murine IgG. In human samples, it was shown that 15-25% of the Fab IgG part is wearing *N*-glycans on a hypervariable region, close to binding site (Figure 4.). They affect antibody-antigen association, affinity maturation, effector functions and are prone to modifications during pregnancy (Bondt *et al.*, 2016; van de Bovenkamp *et al.*, 2018). Also, some studies show that the Fab *N*-glycosylation contributes to diversity of binding sites. Naive human B-cells contain only few Fab alleles that can express sites for *N*-glycosylation. Therefore, most of the glycan-sites present on the hypervariable domain probably appear as a result of somatic hyper mutation (SHM) during the immune response induced by encounter with the antigen. This is mostly noticed on human samples while it still remains unclear for the mouse IgG (van de Bovenkamp *et al.*, 2016; van De Bovenkamp *et al.*, 2018).
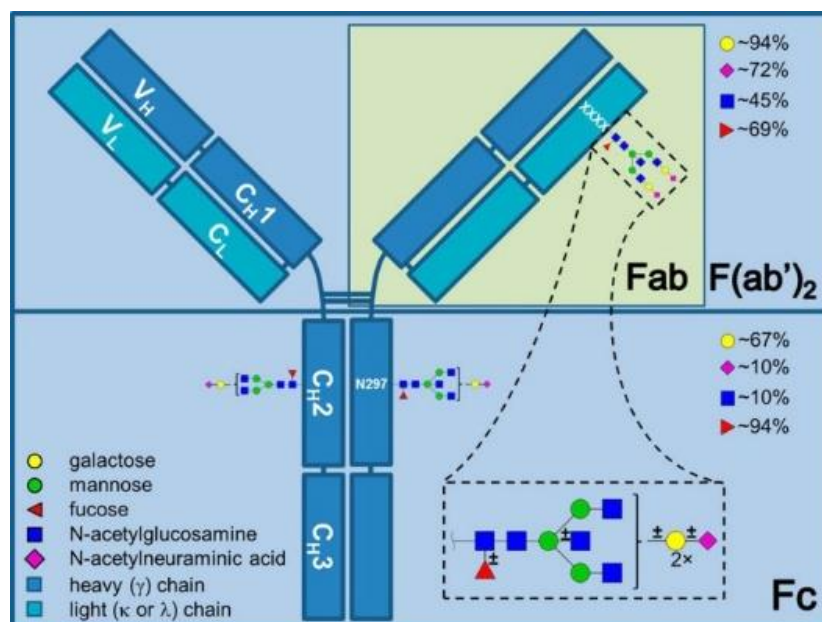
Figure 4. IgG *N*-glycosylation sites on Fc and Fab region (Bondt *et al*., 2014).

1.2.3. Genetic control of immunoglobulin structure

The V domains of HCs and LCs are encoded by *V(D)J* gene segments, while individual exons (part of a gene that will encode a part of the mRNA after removing of non-coding parts) are coding C domains. The V domain sequence is divided into three CDR regions placed

between four regions of a stable sequence (framework regions, FRs)(Schroeder and Cavacini, 2010).

The structure of this segment has been well described for the human IgG. The *V* gene segment is organized in a way that it has a promoter (a sequence of DNA to which proteins bind that initiate transcription of a single RNA), a leader exon, an intervening exon, an exon which encodes first three FRs, CDR1 and 2, an amino-terminal end of CDR2, and a recombination signal sequence (RSS). The joining (*J*) gene segment begins with the carboxyl-terminal end of CD3 which is also a recombination signal for this segment. Also, the FR4 is included in *J*.

The RSS has a conserved sequence *CACAGTG* and a less conserved 9-bp *ACAAACCC*. These sequences are separated by 12-23 bp which will direct nonamer and heptamer sequences on the same side of DNA, but will be separated by 1-2 helix turns. A 1-RSS spacer made from 12-bp preferably recognizes a 2-RSS spacer made from 23-bp. Likewise, the *V-V* or *J-J* rearrangement is prevented (Schroeder and Cavacini, 2010).

For a successful *V(D)J* recombination recombination activating genes (RAGs) 1 and 2 are necessary. They initiate Non-homologous end joining (NHEJ) proteins (Ku70, Ku80, DNA-PKcs, Artemis, XRCC4 and ligase) to repair breaks between *V(D)J* and the RSS (Schroeder and Cavacini, 2010).

Genes for HCs and LCs are placed on different chromosome locations. The κ locus is located on chromosome 2p11.2. Variable domains of the kappa chain are made from gene products of *V*κ and *J*κ elements, while the constant kappa domain is encoded by a single Cκ exon. A *VJ* junction of this area designates CDR3 on the κ light chain. The position of the λ locus is on chromosome 22q.11.2 and it assembles four Cλ exons (each associates with his own *J*λ) and three different clusters of *V*λ genes. The HCs form complex with the immature λ chain, known as the ΨLC (pseudo-light chain, surrogate light chain). Together, they form a pre-B cell receptor during the B cell development. The region of the ΨLC gene codes for the CDR3 in light and heavy chain in the pre-B cell receptor. In that way, it enables the B cell to avoid an antigen-specific selection (Schroeder and Cavacini, 2010).

The heavy chain locus is positioned on the chromosome 14q32.33. Roughly 80 V_H genes near chromosome telomere and divided into 7 families encodes the HC. The V_H gene segment includes FR1, FR2, FR3, CDR1, CDR2 and amino-terminal part of the CDR3. There are also diversity heavy chain (D_H) genes segments on this locus. They form the middle of the CDR3 and a whole FR4. Random combination of V_H, D_H and J_H gene segments can bring out 10^7 *V(D)J* combinations.

Altogether somatic variation in the CDR3, individual gene segment, rearrangement and association between different LCs and HCs can give a 10^{16} different immunoglobulin receptors on B-cells (Schroeder and Cavacini, 2010).

Along with the gene diversity and after the encounter with the antigen, variable domain genes undergo somatic hypermutation (SHM). Two main mechanisms are included in this process. The first one refers to mutation hotspots in the purine G/pyrimidine A motif (*RGYW*). The other one is based on an error-prone DNA synthesis which can direct the nucleotide mismatch between the original template and a mutated DNA strand. The gene conversion in the *V* sequence, which contributes to heterogeneity, is possible in other species. The SHM enables affinity maturation of an antibody repertoire after a repeated antigen exposure (Schroeder and Cavacini, 2010).

1.3. IgG *N*-glycosylation in mouse and humans

1.3.1. Variation in *N*-glycan structure during immune response

Studies about IgG glycosylation and how do different pathological conditions affect the IgG glycoprofile started in the 1970's. Since then, glycobiology has evolved as one of the promising approaches in personalized medicine. Today, it is known that not only do different diseases cause alterations in the IgG *N*-glycans structure, but also that the glycoprofile of every individual is prone to changes and can present bigger or smaller risk for developing some illnesses. So far, it is known that inflammation correlates with a decreased galactosylation and an increased bisecting GlcNAc (the GlcNAc between two branches in glycan structure). Probably, the most outstanding glycan change is sialylation with a strong anti-inflammatory effect (Cobb, 2019). Lack of core-fucose is known to significantly (up to 100-fold) increase the affinity of IgG for FcγRIIIA, thereby rendering such antibodies more potent in the induction of the ADCC (Ferrara *et al.*, 2011; Shields *et al.*, 2002). When the level of total serum IgG is observed, up to 35% is mono- or agalactosylated, and about 15% is digalactosylated. Between 10-15% of IgG *N*-glycans are sialylated. Whilst only 10-15% of the *N*-glycans has a bisecting *N*-acetylglucosamine, 90% of the glycans has a core fucose attached to the first *N*-acetylglucosamine (Gudelj *et al.,* 2018). An individual has differently glycosylated IgG variants throughout their life time depending on age, gender, hormones and pathophysiological condition. On a molecule level, the *N*-glycans diversity comes out as a result of the asymmetric glycosylation (different glycans on C_H2 domains on same IgG), new glycosylation sites that are

set during somatic hypermutation, variable composition of monosaccharides, and different *N*-glycan distribution among all four IgG subclasses. Although particular glycan modifications are observed in correlation with some health conditions, it is not completely precise to say that some of them are exclusively pro-inflammatory and the other anti-inflammatory markers (Gudelj *et al*, 2018).

The galactosylation of the *N*-glycans is mostly stable in every individual throughout their lifetime, but also noticeably changes in the state of acute inflammation and during the aging process. The galactosylated Fc *N*-glycans mediate binding to an FcγRIIB inhibitory receptor and are crucial in the anti-inflammatory signaling cascade. They also inhibit pro-inflammatory effects of a complement component C5a (Karsten *et al.*, 2012). Besides that, it is assumed that less galactosylated glycans act pro-inflammatory by interfering with the activation of a complement via lectin (carbohydrate-binding proteins that cause agglutination of particular cells or precipitation of glycoconjugates and polysaccharides – they are involved in cell recognition) and alternative pathways (Gudelj *et al.*, 2018). A similar observation was discovered in the studies on rheumatoid arthritis patients, who had notably agalactosylated IgG. Outstanding variations are also detected in pregnancy. There is an assumption that the IgG *N*-glycans driven, by high estrogen levels during these conditions, are more galactosylated, especially those on the Fc part. Regarding that, decreased galactose levels are observed in the process of menopause when estrogen level is lower (Bondt *et al.*, 2014). However, a galactose molecule on the terminal part of the glycans can mediate a CDC by helping the IgG in Cq1 binding and pathway activation. Furthermore, galactosylated glycans can enhance the association between the Fc fragment of the IgG and FcγRs which can result in ADCC. Both CDC and ADCC are inflammatory processes (Gudelj *et al.*, 2018; Cobb, 2019).

As previously mentioned, sialylation of glycans showed to have a strong anti-inflammatory effect. It is often connected with the process of galactosylation in certain conditions. For example in studies of rheumatoid arthritis pregnant patients, it was shown that women had highly sialylated and galactosylated IgG *N*-glycans during pregnancy (Bondt *et al.*, 2014). This could be an immunosuppressive mechanism because of the potential danger in recognizing fetus as allograft with mismatched antigens (Cobb, 2019). Sialic acid on the Fc part *N*-glycans can moderate a final immune response by means of binding on receptors. If the IgG Fc is sialylated, it will have a lower affinity for the FcγRs expressed in immune cells. Furthermore cells produce pro-inflammatory cytokines (small cell-secreted proteins which participate in cell signaling), the IgG which is highly sialylated while binding to FcγRs (FcγRIIIA) is even lower and causes

both anti-inflammatory effects and reduced ADCC (Gudelj *et al.,* 2018). Also, some studies indicate an interference with lectin binding properties which results in lower sensitivity of adaptive and innate immune cells. This is yet to be explained, as well as the effect of terminal sialic acid residues on the C1q binding and pro-inflammatory response which includes CDC (Gudelj *et al*, 2018). On the other side, interesting observations come from the IgG *N*-glycan analysis from mice with ovarian tumour, where increased sialylation and branching was noticed. Additionally, when the same mice were exposed to pro-inflammatory drugs, sialylation level also increased (Saldova *et al.*, 2013).

The fucose residue in core of *N*-glycan is usually associated with a reduced affinity of IgG to FcγRs (FcγRIIIA and FcγRIIIB), which leads to the preventing of ADCC. Regarding often researched samples from rheumatoid arthritis patients, it was concluded that core fucosylation is high in individuals with juvenile and adult type disease of chronic rheumatoid arthritis (Gudelj *et al*, 2018; Cobb, 2019).

The core fucosylation is closely connected to the presence of bisecting *N*-acetylglucosamine. It is still not completely clarified whether low level of core fucose is the reason of enhanced immune response and ADCC or is it because of the significant presence of the *N*-acetylglucosamine. Particularly, higher GlcNAc levels are associated with a tendency of binding to the FcγRs (Gudelj, *et al*, 2018).

1.3.2. Main differences in IgG *N*-glycosylation between mice and humans

The IgG glycan structures described in a human and mouse are very similar. The main established differences are in the type of sialic acid residue and the presence of α1-3 galactose bound. Regarding sialic acid, the *N*-acetylneuraminic (Neu5Ac) acid is present in human IgG glycans, while the *N*-glycolylneuraminic acid (Neu5Gc) is present in a mouse. The terminal α1-3 galactose bound in the IgG *N*-glycans was found in mouse samples only. It is still unclear if bisecting GlcNAc is present in mice and to what extent, as well as core fucose residues. Some studies show that fucose is always present in the mouse IgG. On the contrary, others disaffirm the statement that IgG fucosylation is lower in mice than in human (Krištić *et al.*, 2018). Interestingly different mouse and human IgG subclasses show specific glycosylation patterns correlated with their function. For example, IgG2a/b is highly galactosylated and sialylated as well as human IgG1 and IgG3. Although they can be found in different organisms, they are both active in the process of inducing the downstream immune response via the FcRs binding after the encounter with an antigen. This confirms that glycoprofile on a certain IgG form determines its function (Zaytseva *et al.*, 2018).

1.3.3. Isotype and strain specific IgG *N*-glycosylation in mice

From the three subclasses of mouse IgG (IgG1, IgG2, IgG3), the IgG2 subclass is further divided into isotypes a, b and c. This classification is created on the alterations in the FcγRs binding properties (Maresch and Altmann, 2016). There are also some reports on two forms of subclass 1 – IgG1F and IgG1I (de Haan *et al.*, 2017). Certain differences in the activity of certain isotypes are also seen in complement activation and bactericidal activity. The study showed that IgG1 has the lowest movement both in complement activation and opsonophagocytosis, while IgG3 precedes in functional activity (Michaelsen *et al.*, 2004). So far, more is known about the Fc part glycosylation than Fab part in human and mice. Likewise, most of the described isotype-specific characteristics are based on the Fc glycosylation analysis. Outbred and inbred mouse strains can be used in translational studies. Usually, the inbred strains are chosen when there is a necessity to distinguish the genetically determined changes from the environmentally influenced ones in some pathophysiological condition such as cancer. It is because they show less genetic variation than the outbred strains. Changes in the IgG *N*-glycosylation were largely described in BALB/c, C57BL/6 (both inbred strains), CD-1 and Swiss Webster (outbred strains). A broad research by de Haan *et al.* (2017) showed presence of biantennary glycans compounded from core Fuc, Gal (or without) and Neu5Gc in the above mentioned strains. Also, variants without core Fuc, but carrying a bisecting GlcNAc or one more molecule of Gal (α1,3) bound to β-linked Gal were detected. The presence of all IgG subclasses, with some variation in IgG1 forms was confirmed in all four strains. Monoatennary glycans were present as well as hybrid and high mannose glycans. The hybrid glycans were described predominantly on IgG2a and IgG2c with high levels in BALB/c and C57/BL6. There were also elevated hybrid glycans on IgG2b in BALB/c. The bisecting GlcNAc on biantennary glycans was much higher in BALB/c and C57BL/6 compared to outbred strains in all IgG isotypes, except the IgG3 where it was low for all strains. The core fucose was mostly high for all the strains, but on IgG2a and IgG2c in BALB/c and C57BL/6 mice, afucosylated biantennary glycans were noted. Regarding IgG2a and IgG2c, the observed glycoforms were highly similar on both isotypes, making it hard to distinguish major differences between them. High galactosylation levels were seen in C57BL/6 on IgG2a/c and IgG3. BALB/c mice had significantly galactosylated IgG3 as well. As sialylation is often connected to galactosylation levels, analysis showed much the same results. The analysis showed the IgG3 carrying more sialylated (Neu-5Gc) N-glycans in C57/BL6 and BALB/C mice compared to CD-1 and in

general, carrying significantly sialylated glycans on IgG2a/c in C57/BL6 mice. Conclusively, through subclasses, the galactosylated glycans were predominantly present in IgG2 isotypes. The level of sialylated glycans was the highest in IgG2 (b). As afucosylated glycans showed more variations, it was more valuable to highlight these differences. It is noted that the biggest data percent for afucosylated structures is on IgG1 subclass. The bisecting GlcNAc in biantennary glycans had the highest level on IgG3 (de Haan *et al.*, 2017). Based on a diverse set of mouse strains, more studies obtained similar results regarding residues ratio – strains with a low level of galactose usually had a low level of sialic acid. Additionally, it was shown that strains with mostly agalactosylated glycans also have a small level of glycans with two galactose molecules (Krištić *et al.*, 2018). An earlier study on samples from BALB/c and C57/BL6 strains confirms the state of mostly fucosylated *N*-glycans, but did not show a significant amount of bisecting GlcNAc and α1,3-galactose (Maresch and Altmann, 2016). Using a high-throughput quantification method, Zaytseva *et al.*, 2018. also showed a presence of fucosylated biantennary *N*-glycans with sialic acid (Neu5Gc) and galactose (or without) on antennae terminal part among all subclasses of the mice IgG (strains C57BL/6, BALB/c and C3H). A low level of α1,3-galactose and prominent amount of agalactosylated glycans was confirmed for the IgG1 subclass. Contrary to the previous study, IgG1 showed the highest level of bisecting GlcNAc. The *N*-glycans on the IgG2 subclass are described as mostly galactosylated and sialylated for all three isotypes. The same study presents a variation among the used strains in glycan residues. The IgG1 in C3H strain deviates with a low level of agalactosylated glycans with bisecting GlcNAc and a less expressed sialylation. The C57/BL6 strain has the unusually lowest level of both galactosylated and agalactosylated glycans on IgG2 isotypes, while sialylation is the highest compared to BALB/c and C3H mice. Alpha 1,3-galactose was the highest in BALB/c strain. The IgG3 was shown to be the most galactosylated in C3H and the most sialylated in C57/BL6. The BALB/c strain in IgG3 carries more agalactosylated glycans, and it is also weakly sialylated considering C57/BL6 and C3H (Zaytseva *et al.*, 2018). In the comparison of samples by gender from the strain heterogeneous sample group, glycans from female samples were more galactosylated and digalactosylated. The male glycans were noticeably more sialylated, had more bisecting GlcNAc and were the mostly agalactosylated glycans (Krištić *et al.*, 2018). Earlier study supports the state of more galactosylated glycans in female mice, which also have more core fucose, sialic acid (α2,6), and largely high mannose glycans when compared to male individuals. In male mice, the α2,3 and branching sialic acid was predominantly present. This study also reveals a bigger difference

in glycosylation pattern in outbred strains than in inbred ones, which suggests a strong genetic impact (Reiding *et al.*, 2016).

1.3.4. IgG Fab and Fc *N*-glycosylation

So far the Fc part of IgG has been broadly researched regarding its *N*-glycosylation. Conserved Asn-297 sites in the CH2 region of IgG are well-known for attached glycans. Mostly, they are complex biantennary type *N*-glycans compounded from the basis of Man3GlcNAc2 and residues core fucose, galactose, (bisecting) *N*-acetylglucosamine, and sialic acid (Neu5Ac/Neu5Gc) (Cobb, 2019). Furthermore, the majority of differences and characteristics of the *N*-glycans which impact an immune response or physiological conditions in general, refer to the Fc part glycosylation features. Also, the described strain and overall isotype variations in mice came from the Fc *N*-glycans analysis. Yet, it would be incorrect to ignore the effect of *N*-glycans which are present on the Fab, and therefore take part in contacting the antigen (van de Bovenkamp et al., 2016).

It is noted that the Fab glycans are present in 15-25% of circulating IgG in serum. The majority of them are complex biantennary type molecules bound to glycosylation sites, which appear during somatic hypermutation (van de Bovenkamp et al., 2016). Both κ and λ constant regions do not have an encoded sequence where glycans could attach. As their presence is detected on the LCs, they are presumed to be linked to variable regions of the HCs and the LCs (Leibiger et al., 1999). Besides their effect on the antigen binding properties via epitope recognition and the IgG half-life, the Fab *N*-glycans were analyzed for some conditions in which their changes were already described. A study on anti-citrullinated protein antibodies (ACPA-IgGs) showed a high amount of the Fab *N*-glycans. The ACPA are specific for rheumatoid arthritis patients and are connected with disease pathogenesis. The structure analysis showed they are largely sialylated. Still, according to this observation, it should be underlined that the standard IgGs from the same patients showed much less Fab *N*-glycans (Hafkenscheid et al., 2017). The sialylation of the Fab *N*-glycans has also been researched. One study shows that cleaving sialic acid from the Fab *N*-glycans causes a loss of IgG anti-inflammatory activity (Käsermann et al., 2012). On the contrary, there are opposite informations, stating a loss of the IgG anti-inflammatory characteristics under a high level of sialylation in mouse (Guhr et al., 2011). Also, there is some evidence of the influence of sialylated Fab *N*-glycans on cytokine production – glycans with a high level of sialic acid initiated the release of prostaglandin E2 from monocytes, which inhibited the production of IFN-α (a cytokine produced by the inner

immune system cells in response to an environmental exposure or a viral infection) (Wiedeman et al., 2013). Furthermore, pregnancy is connected with changes in Fab *N*-glycans also. High levels of progesterone impact the *N*-glycosylation changes of the Fab. This may affect the acceptance of the fetal allograft (Bondt et al., 2014).

Nevertheless, a recent study emphasizes an important role of the Fab *N*-glycans during an antigen specific immune response. It shows that glycosylated *N*-glycans are preferably chosen because they are more stable and have a significant role during SHM. Exact mechanism is yet to be explained (van de Bovenkamp et al., 2018).

1.4. Capillary gel electrophoresis with laser-induced fluorescence

The *N*-glycans in this research were analyzed by performing a capillary gel electrophoresis with laser-induced fluorescence (CGE-LIF) using a DNA sequencer. The CGE-LIF method provides fast and high sensitive glycan analysis. Furthermore, it has the advantage of high throughput analysis, which is convenient when there is an aim to process a bigger set of samples. It is mostly used for the analysis of proteins, peptides, nucleic acids and small organic molecules like hormones, plant metabolites, inorganic ions, etc.

The basic principle of this method is the travel of charged molecules in the electrolyte solution under a high-potential electric field in a narrow capillary towards a positive electrode. The signal from fluorescently labelled molecules is identified on an on-column detector (Zhu, Lu and Liu, 2012). A typical instrument contains a single capillary with the temperature control of capillary and solutions. In order to have a bigger throughput, the instrument can contain up to 96 capillaries (an instrument with 4 capillaries was used for this experiment). The capillaries load samples from a 96-well plate following specific injection protocols depending on the desired signal intensity (Lu *et al.*, 2018).

Since polysaccharides do not have chromophores (molecules that absorb particular wavelengths of visible light), they cannot be detected with an absorbance detection in ultraviolet spectrum. That is why a fluorophore is added when performing the CGE-LIF. Labelling of the *N*-glycans is relatively simplified by targeting the reducing end of polysaccharide structures (Figure 5.). For this purpose, 8-aminopyrene-1,3,6-trisulfonate (APTS), which has an excitation maximum near 488 nm line of an argon ion laser, is used. In this way, the *N*-glycans are covalently modified in the reaction of reductive amination which covers almost 100% of labelled molecules (Lu *et al.*, 2018)
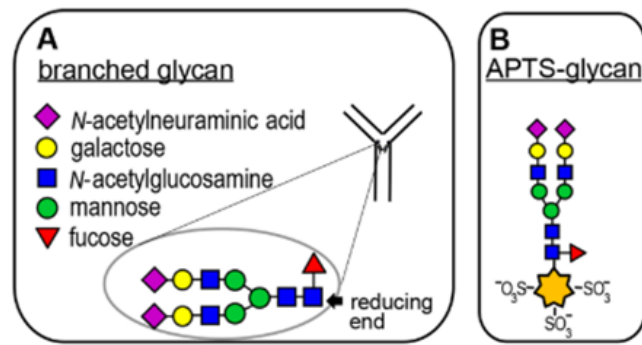
Figure 5. APTS-labelled glycan (Lu *et al.*, 2018).

2. Research aim

So far, many studies confirming the influence of *N*-glycosylation on proteins have been published. IgG is the most abundant protein in serum, and the most explored glycoprotein. It is broadly researched with the aim to elucidate the potential role of its structural changes, including a differential *N*-glycosylation, in disease development. *N*-glycans on the Fc part of the IgG were thoroughly analyzed both in mouse and human. They showed significant associations with various physiological and pathological conditions. Logically speaking, researching the role of the Fab *N*-glycans was the next step. The first results on the *N*-glycosylation of the Fab region of IgG indeed showed the importance of structural changes based on the differential IgG glycosylation for the function of IgG. Similarly to the Fc region, changes in the Fab *N*-glycosylation pattern were observed in association with several diseases. However, unlike in the Fc region, the level of the *N*-glycosylation on the Fab domain was also changed in some of those pathological states. These findings sparked an interest in Fab glycosylation and encouraged the development of methods for its analysis.

As a source of IgG, the human blood serum is an easily accessible biological sample. It is routinely collected in observational and epidemiological studies. However, studying the human IgG *N*-glycosylation changes in most informative and interventional studies *in vivo*, is mostly not possible due to reasonable ethical limitations. To circumvent this, mice models are often employed. Indeed, various mice strains have already served as good IgG *N*-glycosylation models for human IgG because of their similarity in the IgG structure, function, and glycosylation as well as in FcγR signaling. However, the Fab *N*-glycosylation data, as well as the data on the comparison of the *N*-glycan content between the Fab and the Fc regions in mice, is scarce compared to the human IgG. Additionally, slight structural differences in the peptide part of the molecule and the mild differences in the IgG *N*-glycan composition require an optimization of analytical methods for the glycoanalysis of the mouse IgG.

Therefore, the aim of this study was to establish the analytical method for the exploration of the mouse Fab and the Fc glycosylation based on the method used for the human IgG. As a proof of concept, the method was to be used for an initial comparison of the mouse Fab and the Fc glycopattern. Once developed and optimized, the method will be used in future studies involving the mouse Fab and the Fc glycosylation.

3. Materials and methods

3.1. Materials

3.1.1. Mice

As a source of IgG, blood serum from CBAT6T6 mouse strain was used (Table 1.). Animals were bred in the Animal Facility at Division of Animal Physiology, Department of Biology, Faculty of Science, University of Zagreb and their use was approved by Croatian Ministry of Agriculture for teaching purposes (Registry number: 525-10/0529-17-8; see Chapter 8.).

Table 1. Animal sample information

Animal	mouse
Strain	CBAT6T6
Age	130 ± 10 days
Gender	male
Weight	29.5 – 37.07 g (av. 34.45 g)
Number of sampled animals	12

3.1.2. Inorganic chemicals

Table 2. Inorganic chemicals

Chemical	Manufacturer
Disodium hydrogen phosphate ($Na_2HPO_{4(s)}$)	GRAM MOL
Potassium dihydrogen phosphate ($KH_2PO_{4(s)}$)	BIOCHEM Chemopharma
Potassium chloride ($KCl_{(s)}$)	GRAM MOL
Sodium chloride ($NaCl_{(s)}$)	ALKALOID AD Skopje
Ammonium bicarbonate ($NH_4HCO_{3(s)}$), 0.1 M	Sigma-Aldrich
Sodium hydroxide ($NaOH_{(s)}$), 0.1 M	MERCK

3.1.3. Organic chemicals

Table 3. Organic chemicals

Chemical	Manufacturer
2-mercaptoethanol ($C_2H_6OS_{(l)}$)	ACROS ORGANICS
Ethanol ($C_2H_5OH_{(l)}$) anhydrous, EtOH	Sigma-Aldrich
TRIS ($C_4H_{11}NO_{3(s)}$), (2-Amino-2-(hydroxymethyl)propane-1,3-diol)	Sigma-Aldrich
SDS ($NaC_{12}H_{25}SO_{4\,(s)}$), (Sodium dodecyl sulfate)	Sigma-Aldrich
2-PB ($C_6H_7BN_{(l)}$), (2-picoline borane)	Sigma-Aldrich
DMSO ($C_2H_6OS_{(l)}$), (Dimethyl sulfoxide)	Sigma-Aldrich
Citric acid monohydrate ($C_6H_8O_7 \times H_2O_{(s)}$), CA	Sigma-Aldrich
Formic acid (CH_2O_2) 0.1 M, pH 2.5	HONEYWELL
APTS ($C_{16}H_8NNa_3O_9S_{3(s)}$), 8-Aminopyrene-1,3,6-trisulfonic acid trisodium salt	Sigma-Aldrich
4% Igepal (($C_2H_4O_n)C_{14}H_{22}O_{(l)}$), Octylphenoxy poly(ethyleneoxy)ethanol	Sigma-Aldrich
Triethylamine ($C_6H_{15}N_{(l)}$), TEA	Sigma-Aldrich
Acetonitrile ($CH3CN_{(l)}$) (HPLC grade), ACN	HONEYWELL
Acetic acid ($CH_3COOH_{(l)}$)	Sigma-Aldrich
Narketan anesthetic	Vetoquinol S.A., BP 189 Lure Cedex
Xylapan anesthetic	Vetoquinol Biowet Sp.

3.1.4. Biological chemicals

Table 4. Biological chemicals

Chemical	Manufacturer
PNGase F (Peptide *N*-glycosidase F)	Promega
SpeB protease enzyme (SpeB protease enzyme)	Genovis

3.1.5. Solutions and buffers

Table 5. Solutions and buffers

Chemical	Preparation
1 M ammonium bicarbonate	For 100 ml of solution, I mixed 7.9 g of NH$_4$HCO with 100 ml of mqH$_2$O. Buffer was stored at room temperature.
20% Ethanol in 20 mM TRIS + 0.1 M NaCl, pH 7.4	For 500 ml of solution, I mixed 100 ml of C$_2$H$_5$OH with 1.21 g of TRIS and 2.922 g of NaCl. Then I filled up the solution with mqH$_2$O to volume of 500 ml in a beaker. After dissolving, I settled pH using buffer standards and filtered the solution.
2% Sodium dodecyl sulfate (SDS)	I dissolved 2 g of SDS in 100 ml of mqH$_2$O. Solution was stored at 37°C.
30% Propanol (CH$_3$(CH$_2$)$_2$OH)	For 0.5 l, I mixed 150 ml of 2-propanol and 350 ml mqH$_2$O, and then filtered the solution.
0.1 M NaOH	For 0.5 l of solution I dissolved 2 g of NaOH$_{(s)}$ in 0.5 l mqH$_2$O. Solution was stored at room temperature.
1x PBS (Phosphate-buffered saline), pH 7.4	For 100 ml of solution, I mixed 10 ml of 10x PBS with 90 ml of mqH$_2$O. I settled pH using NaOH and filtered the solution. Buffer was stored at 4°C.
5x PBS (Phosphate-buffered saline), pH 6.6-6.8	For 100 ml of solution, I mixed 50 ml of 10x PBS with 50 ml of mqH$_2$O.
10x PBS, (Phosphate-buffered saline) pH 6.6	For 100 ml of solution I dissolved: 8.0028 g NaCl, 1.3832 g Na$_2$HPO$_4$, 0.2964 g KH$_2$PO$_4$ and 0.1976 g KCl in 100 ml mqH$_2$O. After dissolving, I filtered solution was. Buffer was stored at room temperature.
3.6 M Citric acid solution (CA)	For 25 ml of solution 18.91 g of CA I weighted and added in a glass beaker (50 ml) with 15 ml of mqH$_2$O and magnetic stirrer. I mixed the solution until CA has had completely dissolved. Then, I transferred solution to a graduated cylinder and filled up to 25 ml with mqH$_2$O. Afterwards, I transferred it to a small glass bottle (50 ml). Solution was stored at 4°C.

30 mM in APTS in 3.6 M citric acid	For 1.6 ml of solution, I added 1.6 ml of 3.6 M CA directly into a supplier tube with 25 mg of APTS. I made aliquots of 220 µL and stored them in 0.5 ml tubes. I sealed the tubes with Parafilm and aluminium foil. For one plate of samples (96 well), 220 µL was enough. Aliquots were stored at -20°C.
80% acetonitrile	For one sample a total of 500 µL solution was needed throughout the procedure. To get 80%, I mixed 400 µL of ACN with 100 µL of mqH$_2$O. After preparation, I stored the solution at 4°C.
80% acetonitrile + 100 mM triethylamine, pH 8.5	For total of a 500 ml of solution, I put 400 ml of ACN and magnetic stirrer into a glass beaker (500 ml). Then I added 6.295 ml of TEA and after it 1.2 ml of acetic acid. I set pH to 8.5. I transferred the solution to a graduated cylinder and added mqH$_2$O up to 500 ml. I covered the cylinder with Parafilm and carefully shaked it by holding it with both hands. After shaking, I poured the solution to a glass bottle (500 ml) and stored at 4°C. Before using it, I stirred the solution once more.
pH buffer solution, alkaline standard for pH meter, pH: 9.21	Mettler Toledo GmbH
pH buffer solution, acidic standard for pH meter, pH: 4.01	Mettler Toledo GmbH
pH buffer solution, neutral standard for pH meter, pH: 7.00	Mettler Toledo GmbH
Bio-Gel P-10 slurry (100 mg/ml)	For 200 ml of solution I mixed 20g of Bio-Gel P-10, 140 ml mqH$_2$O, 40 ml ACN and 20 ml EtOH. Solution is stored at 4°C.
Loading dye (5X): 10% SDS + 0.4M Tris pH6.8 + 50% glycerol + Bromophenol blue in mqH2O	SDS: Sigma-Aldrich

3.1.6. Other chemicals
Table 6. Other chemicals

Chemical	Manufacturer
Prestained protein ladder	Abcam
NuPAGE MES SDS Running Buffer (20X)	ThermoFisher
GelCode Blue Stain Reagent	ThermoFisher
PR-1 Reconditioning kit	Thermo Scientific
Capture select IgG-Fc (multi-species) Affinity Matrix / Fc beads	Thermo Scientific
Bio-gel P-10	Bio-Rad

3.1.7. Laboratory equipment and consumables
Table 7. Laboratory equipment and consumables

Equipment and Consumables	Manufacturer
Surgical scissors	/
Scalpel	/
Pincettes	/
Pasteur pipettes	/
Sterile needles	/
Disposable sterile syringe with stopper (10 mL)	/
Cotton wool	/
Preparation tray	/
Mini spin centrifuge	Eppendorf
Spectrafuge Mini spin centrifuge	Sigma-Aldrich
Centrifuge 5804	Eppendorf
Millipore vacuum manifold	Merck
Millipore vacuum pump	Merck

NanoDrop 8000 Spectrophotometer	Thermo Scientific
SpeedVac vacuum concentrator/centrifuge/	Genevac / Thermo Scientific (refrigerator trap)
Vortex genie mixer	Scientific industries
Vibration Shaker/Plate shaker	GFL
Single Channel pipette (0-2 μL)	Rainin
Single Channel pipette (2-20 μL)	Rainin
Single Channel pipette (100-1000 μL)	Rainin
Single Channel pipette (20-200 μL)	Rainin
Single Channel pipette (1000–5000 μL)	Rainin
Multi Channel pipette (5–50 μL)	Rainin
Multi Channel pipette (20-200 μL)	Rainin
Multi Channel pipette (100-1200 μL)	Rainin
Oro-Flex I Polypropylene filter plate w/10 μm, 96-well plate - Orochem filter plate	Orochem
StableRak 20 μL pipette tips	Rainin
Racked 200 μL pipette tips	Rainin
StableRak 300 μL pipette tips	Rainin
StableRak 1000 μL pipette tips	Rainin
StableRak 1000 μL filter pipette tips	Rainin
StableRak 200 μL filter pipette tips	Rainin
Small plastic tube (0.5 mL)	MBP
Small plastic tube (1 mL)	Eppendorf
Small plastic tube (1.5 mL)	Eppendorf
Small plastic tube (2 mL)	Thermo Scientific

Falcon tubes (50 mL)	Sarstedt
96-well Protein G Monolithic plate	BIA separations
Oro-Flex I Polypropylene filter plate (96-well)	Orochem
2 mL Collection plate	Waters
1 mL Collection plate	Waters
1 mL Round Collection plate	Waters
PolyProp Mat Caps for Round Plates	Waters
ABgene PCR plate	Thermo Scientific
Fully skirted PCR plate	Thermo
PCR Stripe Tube 0.2 mL 8-tubestrips	Molecular Bioproducts
Thermal Sealing foil	Porvair
Adhesive seal	Thermo Scientific
Plastic box for humid chamber	/
1 mL AgroPrep GHP 0.45 μm filter plate	Pall Corporation
350 μL AcroPrep GHP 0.2 μm filter plate	Pall Corporation
Buffer basins with lids 250 mL	NALGENE
Reagent basin 60 mL	Mettler Toledo
Kimtech Kimwipes	Kimberly-Clark
Cotton tipped applicators	Puritan
White Heavy Duty Labels	AvreryZweckform
Lumo color permanent pen	Staedler
PD-10 Desalting columns	GE Healthcare
Aluminium foil	/
Incubator DNI 30	MRC

Oven DNO 30	MRC
Thermomixer	ThermoFisher
NuPage Protein 4-12% Bis-Tris Protein Gels, 1.0 mm, 12 well	ThermoFisher
Protein Gel Electrophoresis Chamber system	LIFE Technologies
Analytical balance	Ohaus
Technical balance	Mettler Toledo
Heidolph MR 3000 Magnetic stirrer	Sigma-Aldrich
RCT Basic Magnetic Stirrer	IKA
Benchtop pH Meter	Mettler Toledo
Glass Beaker 50 mL	SciLabware
Glass Beaker 500 mL	Sigma-Aldrich
Glass Beaker 250 mL	SciLabware
Glass Graduated cylinder 1000 mL	Witeg Labortechnik GmbH
Glass Graduated cylinder 500 mL	Witeg Labortechnik GmbH
Glass Graduated cylinder 50 mL	Witeg Labortechnik GmbH
Glass Chemical Container Reagent Bottle 500 mL	Duran
Glass Chemical Container Reagent Dark Bottle 500 mL	Simax
Glass Chemical Container Reagent Bottle 250 mL	Duran
Spatulas	/
Small tube rack	/
Falcon tube rack	/
Weighing boats	Lab logistics group Gmbh
Parafilm	Carl Roth
Fume hood	GIMLab

3.2. Methods

3.2.1. Blood collection and serum isolation

Before blood isolation procedure, I weighed mice using a technical balance. Then I injected them with 0.1 ml/10g of anaesthetics combination (Narketan® 75 mg/kg and Xylapan® 10 mg/kg). Proper level of anaesthesia was reached when they did not show any pedal reflex. I placed each mouse dorsal on the preparation tray and smeared the neck part of body with ethanol. I made a straight incision with a scalpel on the axillar region. After the formation of a small skin gap, I made a short incision on the axillar vein and collected blood in a 2 mL tube using a Pasteur pipette. I euthanized mice performing pneumothorax – skin incision on thoracic ventral side and then incision on diaphragm.

I left tubes with blood at room temperature for 10 min and then centrifuged them (10 min, 1620 g), separating serum in the supernatant from the precipitate of blood cells. Using a micropipette, I transferred serum to a new 2 ml tube. Tubes with serum were stored at -20°C until further use.

3.2.2. IgG isolation

The whole isolation procedure was performed in a fume hood. I cleaned all of the used pipettes and the bench surface with water and 70% ethanol, before and after the procedure. 30 min before starting the procedure, I put the solutions and buffers at room temperature.

3.2.2.1. Preparation of serum samples and pre-conditioning of the Protein G plate

As all serum samples were from same mouse strain, age and gender, I pooled them in two 2 mL tubes. I mixed the tubes with serum samples and centrifuged them at 1620 g for 10 min to separate the lipids. Using filtered tips to prevent pipette contamination and avoiding the lipid fraction if there is any, I transferred 100 µL of serum into each of 20 wells of a 2 mL collection plate. I diluted the samples in a plate with 1x PBS in ratio 1:7. Then I transferred the diluted serum into a 1 mL AcroPrep GHP 0,45 µm filter plate. Using a vacuum manifold (maximum pressure), I filtered the samples in a 2 mL collection plate and left on shaker while the Protein G plate was pre-conditioned.

The Protein G plate is stored at 4°C and can be reused, but it should be conditioned before and after every use. All steps of the pre-conditioning and the IgG isolation are performed using a vacuum pump and a vacuum manifold. The pump pressure should not surpass 10 mmHg in the step of applying the serum sample on the Protein G plate and when eluting the IgG. It should not pass 17 mmHg for all the other steps.

Firstly, I removed the storage buffer (20% ethanol in 20mM TRIS + 1M NaCl, pH 7,4) by vacuum to organic waste. I washed each well with 2 mL of mqH₂O and then with 2 mL of 1x PBS to remove possible contamination. To remove the possible remains of IgG on the plate from a previous isolation, I then washed the wells with 0.1 M formic acid. After that, I also washed the wells with 10x PBS for neutralization. I put the Protein G plate on a 2 mL collection plate and washed it with 1x PBS for equilibration before applying the serum. After the washing process, I took 100 µL of 1x PBS from the well A1 in a collection plate, and stored it in a 1.5 mL tube for SDS-PAGE.

3.2.2.2. IgG binding and washing

I transferred the filtered serum samples into a Protein G plate using 1 mL filtered tips to bind the IgG. Using the vacuum, I removed the serum flow-through. Then, I washed the plate three times with 2 mL of 1x PBS. For the process of removing the serum flow-through and all three washes, I put new 2 mL collection plates underneath the Protein G plate. I took 100 µL from the wells A1 in collection plates together with PBS washes and 7 µL from the serum flow-through. Later, I stored them in 1.5 mL tubes for SDS-PAGE.

3.2.2.3. IgG elution

I put the Protein G plate with the bound IgG on top of a new 2 mL collection plate containing 170 µL ammonium bicarbonate (neutralization buffer) per well. In order to elute the IgG using the vacuum in a collection plate (first elution), I added 1 mL of 0.1 M formic acid to the Protein G plate in the wells with the sample. After that, I resuspended the elution samples in the collection plate to prevent the loss of sialic acids because of the acidic conditions. I covered the plate with an aluminium foil and placed it on a shaker. I repeated the elution step one more time. I saved the eluates until determining the concentration of IgG. 100 µL of both eluates from the well A1 were saved in 1.5 mL tubes for SDS-PAGE.

3.2.2.4. Regeneration and storage of Protein G plate

To elute all possible leftover IgG, I added 1 mL of 0.1 M formic acid per well. Then I washed each well of the Protein G plate with 2 mL of 10x PBS and 2 mL of 1x PBS. I washed each well with 1 mL of storage buffer (20% ethanol in 20mM TRIS + 1M NaCl, pH 7,4). The second time I applied the storage buffer, I exposed the plate to the vacuum only for a few seconds so that -most of the buffer stays in the wells. I covered the plate with a plastic lid and stored it at 4°C.

3.2.2.5. IgG concentration measurement and storage

I assessed the IgG concentration by measuring the absorbance at 280 nm in the NanoDrop 8000 Spectrophotometer from each sample (each well from the plates with the first and the second elution) and from the pooled samples later (see Chapter 8.2.). A total volume of the pooled IgG eluates was 23.4 mL and was stored at -20°C.

I saved all collected samples from the wells A1 in different collection plates for the SDS PAGE. I stored the tubes with serum samples and flow-through after IgG binding at -20°C while the IgG washes and eluates I dried in the SpeedVac and then placed them at -20°C until the SDS PAGE.

3.2.3. SDS-PAGE

I used a sodium dodecyl-sulfate polyacrylamide gel electrophoresis (SDS-PAGE) to confirm the presence of the IgG in different fractions collected during the IgG isolation. I also used it to confirm the presence of the Fab and the Fc fractions after a protease digestion in the solution, on the Fc beads, and after the deglycosylation.

I performed the SDS-PAGE on NuPage Protein 4-12% Bis-Tris Protein Gels (1.0 mm, 12 well) with the maximum capacity of 20 µL per well. I diluted the NuPAGE MES SDS Running Buffer (20x) to 1x concentration for use as a running buffer. I always added the protein ladder in the first lane of the gel.

3.2.3.1. SDS-PAGE of fractions collected during IgG isolation

I resuspended stored fractions in 12 µL mqH$_2$O. 3 µL of 5x loading dye (to achieve final concentration of 1x), and I added 0.75 µL of 2-mercaptoethanol from 100% solution for a final concentration of 5% to each sample to cleave disulphide bonds between the heavy chains and light chains of IgG. Since the flow-through samples were in PBS (7 µL), I resuspended them in

5 µL of mqH$_2$O, 3 µL of loading dye and 0.75 µL of 2-mercaptoethanol. To the serum sample (1 µL) I added 11 µL of mqH$_2$O, 3 µL of loading dye, and 0.75 µL of 2-mercaptoethanol.

I denatured the samples for 10 min at 70°C, briefly vortexed and centrifuged (short spin) them. I loaded the total volume of each sample on the gel. 5 µL of protein ladder was loaded in the first well. Electrophoresis was performed at 150 V for 1 hour and 10 minutes. I rinsed the gel then three times with mqH$_2$O and stained using the GelCode Blue Safe Protein Stain. After 1 hour of staining, I destained the gel in mqH$_2$O for 20 hours. I always took gel pictures after 1 hour and after 20 hours of destaining.

3.2.4. IgG desalting

To clean the IgG from ammonium formate and other possible contamination remaining from the isolation procedure, I desalted the IgG eluates using two PD-10 desalting columns. One PD-10 desalting column can desalt 2.5 mL of sample.

3.2.4.1. PD-10 Desalting column preparation and equilibration

First of all, I removed the top caps from both columns and thrown storage buffer (20% ethanol) into organic waste. I cut the sealed end of the column at the notch. I put the columns in 50 mL Falcon tubes to collect the waste. For the process of equilibration, I washed each column four times with 5 mL mqH$_2$O, and emptied by the gravity flow. Then, I added 5 mL of mqH$_2$O and centrifuged the columns at 1000g for 2 min.

3.2.4.2. IgG eluate desalting on PD-10 column

After that, I put the equilibration columns in new Falcon tubes for the collection of the desalted IgG. I slowly added 2.5 mL of IgG eluate to each column. Then, I centrifuged the columns at 1000g for 2 min. Since a single PD-10 desalting column can desalt 2.5 mL of sample, this process was repeated five times to desalt the total of 23.4 mL of IgG.

After use, I put the storage buffer (20% ethanol) in columns which were covered with caps and sealed the column notch. PD-10 columns were stored at room temperature.

IgG concentration measuring and storage

I measured the concentration of the desalted IgG in each of the five Falcon tubes. As the IgG concentration in one of the tubes was negative, likely indicating that all IgG was lost during

the desalting procedure, I pooled the remaining four Falcon tubes with the desalted IgG together. I also measured the final concentration of the pooled samples.

As the total volume of IgG in mqH$_2$O was 20 mL, I aliquoted the samples in 20 small 1.5 mL tubes. I dried the IgG in SpeedVac and stored it at -20°C.

3.3. IgG digestion by SpeB protease

3.3.1. Digestion in solution – testing enzyme activity

To obtain the Fc and Fab fraction of the IgG, I used the SpeB protease enzyme. The SpeB protease is a recombinantly produced cysteine protease which digests antibodies from different species in the hinge region. The enzyme requires reducing conditions for the IgG digestion. The SpeB protease enzyme (FabULOUS, Genovis, Sweden) is stored as a lyophilized powder in the amount of 2000 U, which can digest up to 2 mg of IgG. One unit digests ≥ 95% of 1 µg IgG when incubated in PBS and reducing agent at 37°C for 1 hour (https://www.genovis.com/products/igg-proteases/fabulous/fabulous-enzyme/). Before usage, I resuspended the whole amount of the lyophilized enzyme in 50 µL of water to achieve an enzyme concentration of 40 U/µL. Then I prepared five aliquots of 10 µL enzyme per tube. As a reducing chemical, I used 2-mercaptoethanol to cleave disulphide bonds between the heavy and light chains. By mixing 20 µL of 100% 2-mercaptoethanol with 180 µL of 1X PBS, I prepared 10% solution of 2-mercaptoethanol in a small tube (1 mL) in the fume hood. I performed the process of digestion with the SpeB protease enzyme (1 U/µg IgG) together with 1% 2-mercaptoethanol for 1 hour and 20 hours at 37°C.

By using seven samples of 5 µg of IgG (Table 8.), I tested enzyme activity in the solution for 1 hour and 20 hours of digestion time. I added the SpeB protease enzyme to four tubes from which I exposed two tubes to 1 hour of digestion time and other two to 20 hours of digestion time at 37°C (Table 8). After the 1 hour digestion, I stored the samples at -20°C. One control IgG sample, which did not go through the digestion procedure, was stored at 4°C until the SDS-PAGE (Table 8).

I prepared a total volume of samples and IgG amount per tube accordingly to the SDS-PAGE gel limitations. I resuspended each sample in 1x PBS, and added 2-mercaptoethanol to all of their solutions right before adding the SpeB protease enzyme. For the remaining four samples, I performed the SDS-PAGE after 20 hours of digestion. I added 3 µL of 5x loading buffer (1x final concentration) (Table 8.) to each sample (total volume of 15 µL). As described

previously, I denatured the samples and performed the electrophoresis at 150 V for 1 hour and 10 minutes. The gels were processed as described above (see Chapter 3.2.3.).

Table 8. SpeB digestion in solution testing conditions

Tube	PBS (μL)	10% 2-mercaptoethanol (μL)	SpeB protease 1U/μL (μL)	Incubation temperature	Incubation time
1	13.5	1.5 *	0	4ºC	20 hours
2	13.5	1.5	0	37ºC	20 hours
3	13.5	1.5	0	37ºC	1 hour
4	8.5	1.5	5	37ºC	20 hours
5	8.5	1.5	5	37ºC	20 hours
6	8.5	1.5	5	37ºC	1 hour
7	8.5	1.5	5	37ºC	1 hour

* added before loading on gel to reduce disulphide bonds

3.3.2. Optimization of on-beads digestion conditions

3.3.2.1.   Binding of IgG to Fc beads

I prepared five samples, each containing 25 μg of IgG. A bigger amount of IgG was used in comparison with digestion in the solution due to a potential loss when digested on beads. I used two aliquots as controls. One of them was an undigested IgG placed at 4ºC (for SDS-PAGE) and the second one was an undigested IgG which underwent the entire procedure only without the SpeB protease enzyme (for Fc beads). The process of digestion with the SpeB protease enzyme (1 U/μg IgG) was performed in triplicate. I dried the IgG samples for 3 hours in SpeedVac. I resuspended all samples, except the control sample stored at 4°C, in 100 µl PBS pH 7.4. For the control at 4°C, I took 5 μL from 1 μg/μL aliquote in order to have 5 μg of IgG for the SDS-PAGE.

I shook the Fc beads and resuspended them before pipetting 20 µL in 4 wells of an Orochem filter plate. I placed the plate on a waste container, with which I placed on a vacuum manifold. I washed the beads then four times with 200 µL of 1x PBS. I centrifuged the Orochem filter plate with beads at 50 g for 1 min, and then put on a 1 mL collection plate. I added 25 μg of IgG diluted in 100 µL PBS to the 4 marked wells. I covered the plate then with aluminium foil and incubated it for 1h at room temperature on a plate shaker to make sure the resins bind the Fc part of the IgG. After one hour, I put the Orochem filter plate on a 1 mL collection plate and filtered it using the vacuum manifold.

I put then the Orochem filter plate on a new collection plate and washed four times with 1x PBS, and centrifuged at 50 g for 1 min. After the incubation, I saved the washes and the filtered liquid for the SDS-PAGE. Finally, I covered the plate with an aluminium foil and left it at room temperature, until the chemicals for the next step were prepared.

Digestion of IgG bound to the Fc beads by SpeB

I prepared the SpeB protease enzyme solution (5 U/µL) by mixing 2.5 µL enzyme 40 U/ µL with 17.5 µL PBS. I put a PCR plate under the Orochem filter plate. I added 5 µL of SpeB protease enzyme, 5.5 µL of 10% 2-mercaptoethanol solution (for final concentration 1%), and 24.5 µL PBS pH 7.4 for a total volume of 35 µL to three wells (B1, C1 and D1). To the control (undigested IgG), I added 5.5 µL of 10% 2-mercaptoethanol (for final concentration 1%) and 29.5 µL PBS pH 7.4.

Then I covered the plate with an adhesive seal, and left it on a plate shaker at room temperature for 5 min at medium speed. Then, I incubated it inside the humid chamber at 37°C for 1 hour.

After the incubation, I put together the Orochem filter plate and the PCR plate for the process of shaking for 5 min at medium speed. Then I centrifuged them for 2 min at 50 g to elute the Fab fraction. I put the Orochem filter plate above the waste container and washed it three times with 200 µL PBS (pH 7.4), and three times with 200 µL mqH2O using the vacuum manifold. I centrifuged the plate at 50 g for 1 min to eliminate residual liquid.

In the new PCR plate, I pipetted 17 µL of ammonium bicarbonate to neutralize the Fc elution fraction and thus prevent the loss of sialic acids. Then I put the PCR plate under the Orochem filter plate. I added 100 µL of 100 mM formic acid (pH 2.5) to elute the Fc fragments in the wells with the samples. Together, I left both plates on a shaker for 5 min at a medium speed, and then centrifuged them at 50 g for 2 min.

I assessed protein concentration of the Fc and Fab fractions by measuring the absorbance at 280 nm. I transferred the fractions to 1.5 mL tubes for drying in the SpeedVac for 1 hour.

SDS PAGE

After drying, I performed SDS-PAGE for Fc and Fab fractions, the control sample left at 4°C and for filtrate right after 1h incubation and washes.

To IgG control I added 7 µl mqH$_2$O, 3 µl of the loading dye from 5x solution (for the final 1x concentration) and 1.5 µl of 10% 2-mercaptoethanol (for the final concentration of 1%). I also loaded the SpeB protease enzyme on one lane; I resuspended 25 U of enzyme in 7 µl mqH$_2$O, 3 µl of 5x loading dye (for the 1x final concentration) and 1.5 µl of 10% 2-mercaptoethanol (for the final concentration of 1%).

To washes and filtrates I added 12 µl of mqH$_2$O, 3 µl from 5x solution loading dye (for the 1x final concentration) and 1.5 µl of 10% 2-mercaptoethanol (for the final concentration of 1%).

As described before, I denatured the samples and performed the electrophoresis at 150 V for 1 hour and 25 minutes. The gels were processed as described above (see Chapter 3.2.3.).

3.3.2.1.1. Testing reducing conditions in digestion buffer with 20 hours incubation

Since the process of digestion on the Fc beads for a 1 hour incubation was not as efficient as in the solution with a 1 hour incubation, different concentrations of 2-mercaptoethanol were tested in combination with longer period of incubation (20 hours) in this segment.

I tested a digestion efficacy at different concentrations (0.5%, 1%, 1.5% and 3.5%) of 2-mercaptoethanol in duplicates for digesting 25 µg IgG. I used as controls undigested IgG samples (25 µg), which underwent the whole procedure on the Fc beads (resuspended in 1x PBS pH 7.4, reduced with 2-mercaptoethanol in every tested concentration). I used a single IgG sample as a control for each concentration of 2-mercaptoethanol.

<u>Binding and digestion on Fc beads</u>

As done in the previous section (see Chapter 3.3.2.1.), the binding of IgG samples on beads was performed.

After putting the PCR plate under the Orochem filter plate 1x PBS, I added 2-mercapotethanol and the SpeB protease enzyme according to a total volume of 35 µl (Table 9.).

As done in Chapter 3.3.2.1., I covered the plate with an adhesive seal and left on a plate shaker at room temperature for 5 min at medium speed. Then, I incubated it for 20 hours in a humid chamber at 37°C. I stored the control sample at 4°C for the SDS-PAGE for 20 hours as well.

As described previously (see Chapter 3.3.2.1.), I separated the Fc and Fab fractions and dried them in the SpeedVac for 1 hour.

Table 9. Tested digestion conditions on Fc beads

Sample type with tested 2-mercaptoethanol concentration	10% 2-mercaptoethanol (μL)	PBS pH 7.4 (μL)	SpeB protease 5 U/μL (μL)	Total volume
IgG_0.5%_2-mercaptoethanol	1.75 μL	28.25 μL	5 μL	35 μL
IgG_0.5%_2-mercaptoethanol	1.75 μL	28.25 μL	5 μL	35 μL
IgG_0.5%_2-mercaptoethanol_control	1.75 μL	33.25 μL	0 μL	35 μL
IgG_1%_2-mercaptoethanol	3.5 μL	26.5 μL	5 μL	35 μL
IgG_1%_2-mercaptoethanol	3.5 μL	26.5 μL	5 μL	35 μL
IgG_1%_2-mercaptoethanol_control	3.5 μL	31.5 μL	0 μL	35 μL
IgG_1.5%_2-mercaptoethanol	5.25 μL	24.75 μL	5 μL	35 μL
IgG_1.5%_2-mercaptoethanol	5.25 μL	24.75 μL	5 μL	35 μL
IgG_1.5%_2-mercaptoethanol_control	5.25 μL	29.75 μL	0 μL	35 μL
IgG_3.5%_2-mercaptoethanol	12.25 μL	17.75 μL	5 μL	35 μL
IgG_3.5%_2-mercaptoethanol	12.25 μL	17.75 μL	5 μL	35 μL
IgG_3.5%_2-mercaptoethanol_control	12.25 μL	22.75 μL	0 μL	35 μL

SDS PAGE

I prepared 50% 2-mercaptoethanol by mixing 25 µl of mqH$_2$O with 25 µl of 100% 2-mercaptoethanol. I completely reduced samples by adding 2-mercaptoethanol to a final concentration of 5% before loading on the gel. I resuspended the Fab and Fc samples in 12 µl mqH2O, 3 µl of 5x loading dye (for the final concentration of 1x), and 2-mercaptoethanol. I added 7 µl of mqH2O, 3 µl of 5x loading dye (for final concentration 1x) and 1.5 µl of 50% 2-mercaptoethanol (for final concentration 5%) to the IgG control (5 μg) stored at 4°C before loading on the gel.

As described before (see Chapter 3.2.3.), I denatured the samples and the electrophoresis was first performed at 150V for 50 min, and then at 175V for 20 min because samples were migrating slower than usual. The gels were processed as described above (see Chapter 3.2.3.).

3.3.2.2. Determination of Fc and Fab glycosylation profile of mouse IgG

3.3.2.2.1. IgG digestion

Based on the results obtained during the optimization experiments, the following conditions were used for the final digestion of IgG: 1 U SpeB/µg IgG in reducing conditions (1% 2-mercaptoethanol) with 20 hours incubation at 37°C on 20 µL of the Fc beads for one sample containing 100 µg of IgG. 100 µg of undigested IgG was used as a control sample. In order to save enough fractions of the Fc and Fab for both CGE-LIF and SDS-PAGE, but also to obtain good signal intensity on CGE-LIF, the amount of IgG was increased compared to previous experiments.

I stored two control IgG samples at 4°C, one for the SDS-PAGE (5 µg) and one for the CGE-LIF (20 µg IgG). A control IgG sample (20 µg) was stored at 37°C for the CGE-LIF. After binding on the Fc beads, as described previously, I added 2.5 µL of the SpeB protease enzyme (from 40U/µL solution), 4.5 µl of 10% 2-mercaptoethanol (for the final concentration of 1%) and 28 µL of PBS pH 7.4 to the IgG sample. To the control (undigested) IgG I added 30.5 µl of PBS pH 7.4 and 4.5 µl of 10% 2-mercaptoethanol (for the final concentration 1%). I covered the plate with an adhesive seal and left it on the plate shaker at room temperature for 5 min at medium speed. Afterwards, I incubated it inside the humid chamber at 37°C for 20 hours. I separated the Fab and Fc fractions as described previously (see Chapter 3.3.2.1.).

SDS PAGE

I pipetted 15 % of both eluates (Fc 17 µL, Fab 5 µL) in 1.5 mL tubes for SDS-PAGE, dried and stored at -20°C until processing.

SDS-PAGE was performed like described (see Chapter 3.2.3.). To Fc and Fab samples I added 12 µl mqH$_2$O, 3 µl of 5x loading dye (for final concentration 1x) and 2-mercaptoethanol to have final concentration of 5% (1.2 µL from 50% 2-mercaptoethanol for Fab samples, 1.5 µl from 50% 2-mercaptoethanol for Fc samples). To the mouse IgG control (5 µg, stored at 4°C) I added 7 µl of mqH$_2$O, 3 µl of 5x loading dye (for final concentration 1x) and 1.5 µl of 2-mercaptoethanol (for final concentration 5%).

The remaining percentage after the last digestion was saved in the PCR plate in one column - 35 µL of PBS (Fab is stored in PBS) and 117 µL of ammonium formate (100 µL of formic acid and 17 µL of ammonium bicarbonate, Fc fraction). In wells of the same column I added controls (IgG 37°C, IgG 4°C) and blanks. I dried the samples in the SpeedVac for 2 hours and kept them at -20°C until the PNGase F glycan releasing reaction.

3.3.2.2.2. Deglycosylation

Before the procedure chemicals were allowed to reach room temperature (2% SDS, 4% Igepal and 5x PBS).

For deglycosylation, I prepared 1.66x PBS by mixing 2 mL of mqH_2O with 1 mL of 5x PBS, and 0.5 % SDS by mixing 3 mL of mqH_2O with 1 mL of 2% SDS. The PCR plate with digested samples previously stored at -20°C was allowed to reach room temperature.

I added to the PCR plate with samples, 3 µL of 1.66x PBS per well and then 4 µL of 0.5% SDS per well. I resuspended the samples by pipetting when adding the solutions. I sealed the plate with an adhesive seal and incubated it at 65°C for 10 min. After 10 min, I resuspended the samples with 2 µL of 4% Igepal per sample to prevent the inhibitory effect on the enzyme (PNGase F). I put the plate on the shaker until the enzyme was prepared.

I prepared the PNGase F solution by mixing 1 µL of 5x PBS with 0.12 µL of PNGase F per sample. The solution was prepared for 10 samples (10 µL of 5x PBS with 1.2 µL of PNGase F). I added 1 µL of enzyme solution to each sample in the well. I sealed the plate with a thermal sealing foil and incubated it at 37°C for 3 hours. After the incubation, I dried the samples in the SpeedVac for 1 hour.

3.3.2.2.3. APTS sample labelling

Each of the samples I first resuspended in 2 µL of mqH_2O. I prepared the APTS labelling solution for the samples by mixing 20 µL of APTS labelling solution (30 mM APTS in 3.6 M citric acid) and 20 µL of PB solution (1.2 M 2-picoline borane in DMSO). I put 4 µL of the APTS labelling solution carefully on top of each sample in the well. I sealed the plate with a thermal sealing foil, mixed using vortex for 10 seconds and incubated it at 37°C for 16 hours. I stopped the labelling reaction stopped by adding cold 80% ACN.

I covered the PCR plate with an aluminium foil and put at 4°C until the Bio-Gel P-10 Slurry was prepared.

3.3.2.2.4. Preparation and conditioning of Bio-Gel P-10 Slurry

Bio-Gel P-10 was allowed to reach room temperature before using and gently shaked. Clean 350 µL AcroPrep GHP 0.2 µm filter plate was put on top of the waste container and together I put them on vacuum manifold. I added 190 µL of Bio-

Gel P–10 slurry to each well of the GHP plate and applied the vacuum. Vacuum pressure in all steps of using vacuum manifold cannot exceed over 2 inHg. Then I washed GHP plate three times with 200 µL of mqH$_2$O (1 minute incubation before washing using vacuum manifold). After it, I added 200 µL of cold 80% ACN to wells, held for 1 minute and washed using vacuum and repeated the process two times.

3.3.2.2.5. Clean-up of APTS labelled *N*-glycans

I placed all solutions in buffer basins with lids at room temperature.

I spun the PCR plate with samples and transferred a total volume from wells with samples (106 µL) to the GHP plate containing the Bio-Gel P-10. I shook transferred samples for 5 minutes at 450 rpm using a ThermoMixer. I put the GHP plate on top of the waste container and used the vacuum manifold to discard the flow-through. Next, I added 200 µL of 80% ACN containing 100 mM TEA (pH 8.5). I put the plate on the ThermoMixer (450 rpm) for 2 minutes. After the time spent in the ThermoMixer, I removed the liquid from the plate by the vacuum. I repeated this step four times. Then, I added 200 µL of 80% of ACN, shook on the ThermoMixer (450 rpm) for 2 minutes, and removed it by the vacuum. This step I repeated twice. I spun the plate (quick spin program) and put it on a new 1 mL collection plate. I covered the wells which did not contain samples with an adhesive seal to make stronger sucking pressure.

To elute the APTS-labelled *N*-glycans, first I washed the GHP plate with 100 µL of mqH2O and shook it on the ThermoMixer (450 rpm) for 5 minutes to allow swelling of the particles. By using the vacuum manifold, I collected the flow-through in 1 mL collection plate. When doing the vacuum filtration, I covered GHP plate with a ThermoMixer lid.

To collect the first fraction of the eluate, I added 200 µL of mqH$_2$O to the GHP plate, and shook it on the ThermoMixer (450 rpm) for 5 minutes. Using the vacuum manifold, I eluted the fraction in the collection plate. The same procedure, as the one for collecting the first fraction, I repeated for the second fraction.

I covered the collection plate with eluates (cca 400 µL) with a thermal sealing foil and stored it at -20°C until needed for the CGE-LIF.

3.3.2.2.6. CGE-LIF analysis of *N*-glycans

Before the sample analysis, I assessed signal intensity by the CGE-LIF measurement without the internal normalization. Total volume of the reaction mixture in the well for the CGE-LIF was 10 µL. I pipetted 3 µL of *N*-glycan post-cleanup eluate from the Fc, Fab, and control samples, and 7 µL of HiDi Formamide (Applied Biosystems, USA) into a MicroAmp

Optical 96-well Reaction Plate (Applied Biosystems, USA) and sealed it with a 96-well plate septa (Applied Biosystems, USA). Then I briefly centrifuged a covered plate with the mixture. The CGE-LIF measurement was performed in a DNA Genetic Analyzer (Applied Biosystems, USA) which has four capillaries filled with POP-7 polymer (Applied Biosystems, USA). The sample injection was run at 7.5 – 15 kV for 5 and 10 seconds depending on the signal intensity. A second run was done using 1 µL of the *N*-glycan post-cleanup eluate from the undigested IgG and control samples mixed with 9 µL of HiDi Formamide. The undigested IgG and controls were run for 5 and 10 seconds. In the plate for the CGE-LIF device, I arranged the samples as shown in Table 18. I used 10 µL of HiDi Formamide as a blank chemical for the CGE-LIF and 1 µL of APTS labelled human IgG glycans mixed with 9 µL of HiDi as the standard. Since the device has four capillaries and each one of them can only go in one well, I set a total of six runs.

Table 10. Sample arrangement on plate for CGE-LIF

| HiDi	Fab_undigested	standard
HiDi	Fab_digested	standard
HiDi	Fc_undigested	standard
HiDi	Fc_digested	standard
HiDi	IgG_37°C (20 µg)	HiDi
HiDi	IgG_4°C (20 µg)	HiDi
HiDi	PBS	HiDi
HiDi	ammonium formate	HiDi

3.3.2.3. Data processing

The results were converted from an .abi file to a .txt file and I processed them numerically and graphically in the Empower program (Waters, USA). The analysis is based on the integration of function and separation of the glycan peaks. I analysed unique electropherogram for every sample. Abscissa presents the RT (retention time) expressed in minutes and ordinate defines the RFU (relative fluorescence units) as the *N*-glycan signal measurement. RT is a measure of the time taken for a solute (*N*-glycan) to pass through a chromatography column. RFU are defined as an amount of light collected by the instrument at a given RT. As molecules in samples gave wide spectrum of signal intensity, I limited the signal intensity of observed *N*-glycans from 1000 to 8000 RFU. I set up the base line, which should go right below the electropherogram line, and determined a peak start and an end point for each peak on the electropherogram. Surface area between the electropherogram and the base line that finishes with the start and the end point was defined as the glycan area percentage. Also, a normalized height of each glycan peak was observed and defined as the proportion height percentage (% PHP), a percentage of the total heights of all peaks. PHP was taken as the main distinction feature for each described glycan peak. Finally, I compared glycan peaks data and shown it using Microsoft Office Excel tools.

I annotated glycan content of each peak in control samples (IgG 4°C and IgG 37°C) according to published information (Schaffert et al., 2020).

4. Results

4.1. IgG was successfully isolated from mouse serum

      After IgG isolation from the mouse serum, the SDS-PAGE of washes and both eluates was performed to assess the isolation efficiency. Pictures after 1 hour of destaining are shown due to a better band visibility (Figure 6). The IgG isolation was successful and fairly specific. By assessing the concentration, the final amount of IgG after isolation and before pooling of the samples was calculated to be 93.6 μg in the volume of 1170 μL (average concentration - 0.08 μg/μL). After pooling the samples and assessing their concentration, we calculated that the IgG amount was 1.77 mg (in total volume 23.4 ml). On Figure 6 we see that the vast majority of the IgG is captured in the first elution fraction: in lane 8 (first IgG elution) the heavy chain and light chain bands are visible, while faint heavy and light chain bands are also visible in lane 9 (second elution).
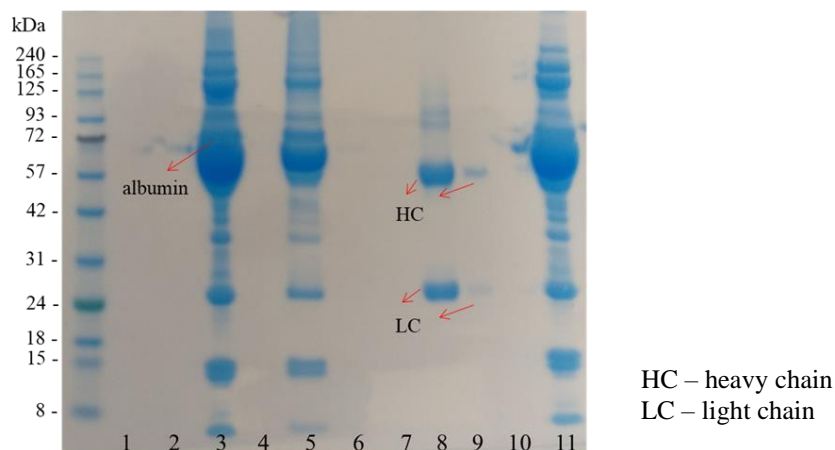
Figure 6. SDS-PAGE separation of serum proteins before the IgG isolation and in different fractions during and after the IgG isolation. 1 – wash before IgG binding; 2 – loading dye; 3 – flow through after IgG binding; 4 – loading dye; 5 – wash 1; 6 – wash 2; 7 – wash 3; 8 – first IgG elution; 9 – second IgG elution; 10 – loading dye; 11 – mouse serum

4.2. IgG medium was exchanged from ammonium formate to mqH$_2$O using PD-10 Columns

      The IgG was successfully desalted from ammonium formate and stored in mqH$_2$O. Nevertheless, some IgG was lost during the procedure. By comparing the assessed IgG concentrations before and after the procedure, the calculated loss through medium exchange was 28%. Total amount of IgG after desalting was 1.271 mg compared to 1.77 mg before desalting.

4.2. SpeB protease enzyme digests reduced IgG in solution after 1 hour incubation at 37°C

In solution, the SpeB protease (1U/μg) cleaved IgG into the Fc and Fab fraction after both 1 and 20 hours of digestion in reducing conditions (1% 2-mercaptoethanol) (Figure 7).
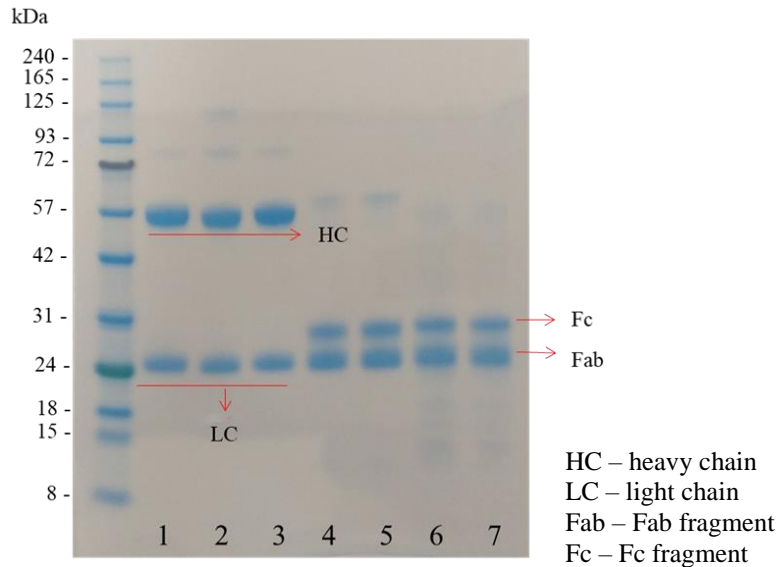
Figure 7. The SDS-PAGE separation on the gel of samples digested by the SpeB protease (1 U/μg IgG) in solution. 1 – IgG at 4°C without SpeB;2 - IgG at 37°C (20 h incubation) without SpeB; 3 - IgG at 37°C (1h incubation) without SpeB; 4,5 – IgG at 37°C (20 h digestion) with SpeB; 6,7 - IgG at 37°C (1h digestion) with SpeB

4.3. IgG was incompletely digested by SpeB protease on Fc beads after 1 hour incubation at 37°C

Digestion of IgG on Fc beads (SpeB protease 1 U/μg IgG, 1% 2-mercaptoethanol, 1 hour) proved digestion was incomplete (Figure 8. and Figure 9).

On Figure 8., lanes 1-3 show an IgG reduced by 2-mercaptoethanol, and lanes 4-7 show that the SpeB protease digests reduced IgG in solution independent of digestion time. In lane 1, the bands from the heavy and light chain are visible confirming the IgG was reduced. The IgG molecule was bound to the Fc beads via Fc fragment. Therefore, there is no bands in lane 2 there and the Fab could not be eluted. The Fab bands in lanes 3-5 and the Fc bands in lanes 7-9 confirm that the SpeB digested some IgG bound to the Fc beads. Although, the faint upper bands in those lanes impose that the IgG was incompletely reduced and digested. In lane 10 the SpeB enzyme band is recognized.

On Figure 9., bands in lanes 1 and 2 suggest IgG presence in the flowthrough as a result of not all IgG molecules binding to Fc beads.
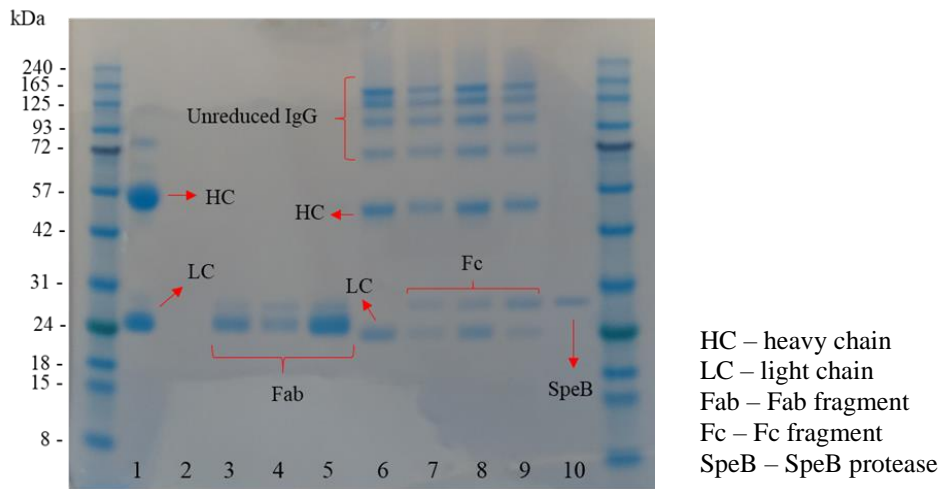
Figure 8. The SDS-PAGE separation on the gel of the Fc and Fab fractions from the reduced IgG digested by the SpeB protease (1 U/µg IgG) on Fc beads (1h incubation at 37°C). 1 – Mouse IgG control 5 µg (4°C), reduced with 1% 2-mercaptoethanol; 2 – Fab fraction of IgG in PBS with 1% 2-mercaptoethanol without SpeB; 3,4,5 – Fab fraction with 1 U/µg SpeB in PBS with 1% 2-mercaptoethanol; 6 – Fc fraction of IgG in PBS with 1% 2-mercaptoethanol without SpeB; 7,8,9 – Fc fraction with 1 U/µg SpeB in PBS with 1% 2-mercaptoethanol; 10 – SpeB protease 25 U.
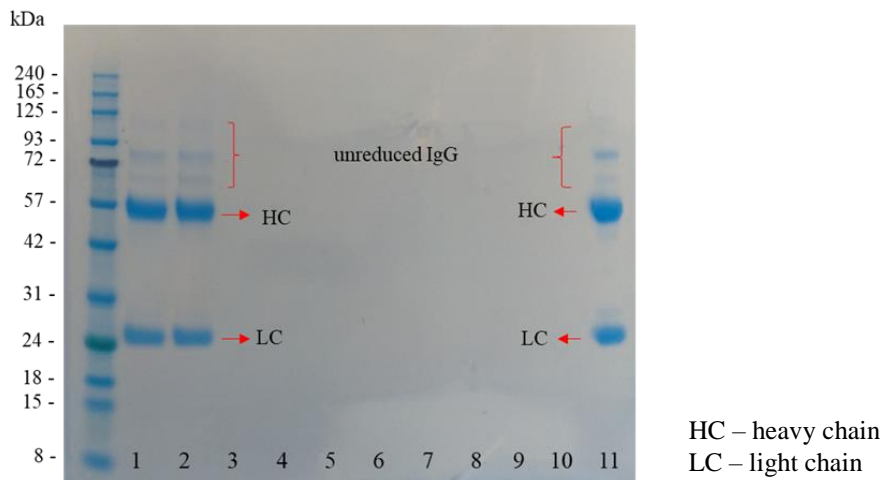
Figure 9. SDS-PAGE separation on gel of flowthrough and washes after IgG binding on Fc beads, duplicate samples. 1,2 – Flowthrough after IgG binding; 3,4 – Wash 1 after flowthrough in PBS; 5,6 – Wash 2 in PBS; 7,8 – Wash 3 in PBS; 9,10 – Wash 4 in PBS; 11 – Mouse IgG control 5 µg (4°C), reduced with 1% 2-mercaptoethanol

4.3.1. Digestion of IgG is efficient after 20 hours incubation at 37°C on Fc beads

After testing the enzyme digestion with the reduced IgG (1% 2-mercaptoethanol) on Fc beads for 1 hour, the SDS-PAGE showed incompletely reduced and partially cleaved IgG in Fc fractions. Considering this results, the incubation period for the digestion of IgG bound to Fc beads, was prolonged from 1 hour to 20 hours and combined with different 2-mercaptoethanol concentrations in the second experiment (Figure 10., 11. and 12.).

On Figure 10., the Fc and Fab bands in lanes 1-10 show that using different 2-mercaptoethanol concentrations does not affect the IgG digestion by the SpeB protease. 20 hours incubation time for digestion of IgG on Fc beads seems to be more effective than 1 hour incubation.

On Figure 11., the Fc and Fab bands in lanes 1-6 again confirm that various 2-mercaptoethanol concentrations do not affect the IgG digestion by the SpeB protease. The heavy and light chain bands in lanes 8 and 11 show that the IgG was reduced by 2-mercaptoethanol in both concentrations but incompletely (faint upper bands). 20 hours incubation time of digesting IgG on the Fc beads shows no difference in IgG digestion with higher concentrations of the reducing agent (lanes 1-6).

The faint upper bands on Figure 12. above the heavy and light chain bands in lanes 2 and 4 imply an incomplete reduction of the IgG, regardless of the used 2-mercaptoethanol concentrations.
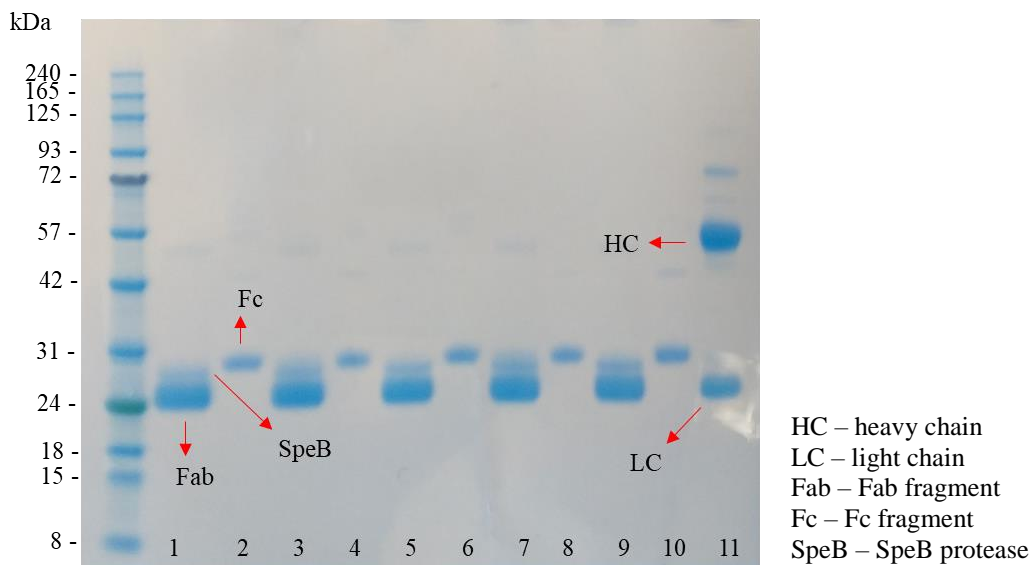
Figure 10. The SDS-PAGE separation on the gel of the Fc and Fab fractions from the reduced IgG digested by the SpeB protease (1 U/µg IgG) on the Fc beads (20 hours incubation at 37°C; 0.5%, 1%, 1.5% 2-mercaptoethanol). 1,3 - IgG digested with SpeB, Fab fraction (reduced on Fc beads with 0.5% 2-mercaptoethanol); 2,4- IgG digested with SpeB, Fc fraction (reduced on Fc beads with 0.5% 2-mercaptoethanol); 5,7- IgG digested with SpeB, Fab fraction (reduced on Fc beads with 1% 2-mercaptoethanol); 6,8 – IgG digested with SpeB, Fc fraction (reduced on Fc beads with 1% 2-mercaptoethanol); 9 – IgG digested with SpeB, Fab fraction (reduced on Fc beads with 1.5% 2-mercaptoethanol); 10 – IgG digested with SpeB, Fc fraction (reduced on Fc beads with 1.5% 2-mercaptoethanol); 11 – IgG (4°C; reduced with 5% 2-mercaptoethanol before loading on gel)

* 2-mercaptoethanol was additionally added to all the Fc and Fab samples before loading on the gel to have the final concentration of 5% of the reducing agent
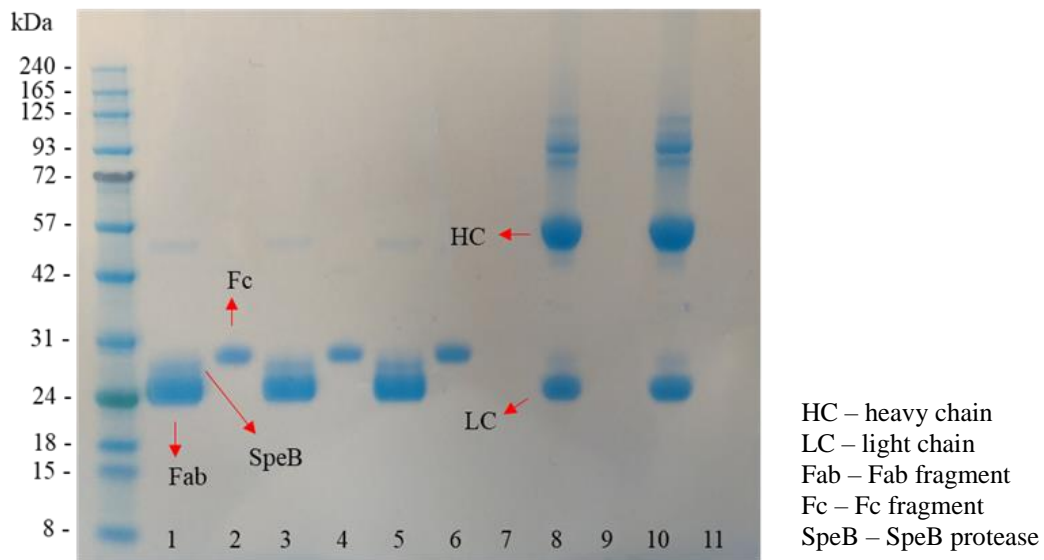
Figure 11. The SDS-PAGE separation on the gel of the Fc and Fab fractions from the reduced undigested IgG and digested IgG by the SpeB protease (1U/μg IgG) on the Fc beads (20 hours incubation at 37°C; 1.5%, 3.5%, 0.5% and 1% 2-me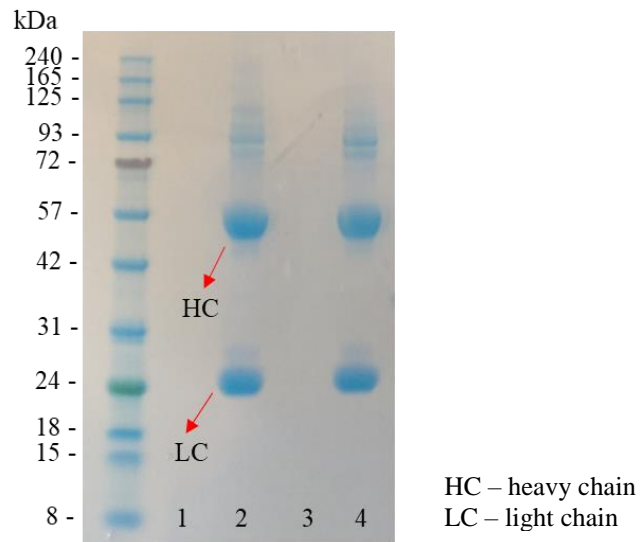rcaptoethanol). 1 - IgG digested with SpeB, Fab fraction (reduced on Fc beads with 1.5% 2-mercaptoethanol); 2- IgG digested with SpeB, Fc fraction (reduced on Fc beads with 1.5% 2-mercaptoethanol); 3,5 - IgG digested with SpeB, Fab fraction (reduced on Fc beads with 3.5% 2-mercaptoethanol); 4,6 - IgG digested with SpeB, Fc fraction (reduced on Fc beads with 3.5% 2-mercaptoethanol); 7 - IgG without SpeB, Fab fraction (reduced on Fc beads with 0.5% 2-mercaptoethanol); 8 - IgG without SpeB, Fc fraction (reduced on Fc beads with 0.5% 2-mercaptoethanol); 9 - IgG without SpeB, Fab fraction (reduced on Fc beads with 1% 2-mercaptoethanol); 10 - IgG without SpeB, Fc fraction (reduced on Fc beads with 1% 2-mercaptoethanol); 11 – loading dye

* 2-mercaptoethanol was additionally added to all the Fc and Fab samples before loading on the gel to have the final concentration of 5% of the reducing agent

*Figure 12.*The SDS-PAGE separation on the gel of the Fc and Fab fractions from the reduced undigested IgG on the Fc beads (20 hours incubation at 37°C; 1.5% and 3.5% 2-mercaptoethanol). 1 -IgG without SpeB, Fab fraction (reduced on Fc beads with 1.5% 2-mercaptoethanol); 2 - IgG without SpeB, Fc fraction (reduced on Fc beads with 1.5% 2-mercaptoethanol); 3 - IgG without SpeB, Fab fraction (reduced on Fc beads with 3.5% 2-mercaptoethanol); 4 - IgG without SpeB, Fc fraction (reduced on Fc beads with 3.5% 2-mercaptoethanol)

* 2-mercaptoethanol was additionally added to all the Fc and Fab samples before loading on the gel to have the final concentration of 5% of the reducing agent

4.4. PNGaseF successfully released *N*-glycans

Considering the described results, 20 h incubation period (at 37°C) on the Fc beads was used in combination with the SpeB enzyme (1U/μg IgG) and 1% 2-mercaptoethanol for the final digestion reaction before the process of deglycosylation and the CGE-LIF *N*-glycan analysis.

The SDS-PAGE was performed to confirm a successful digestion of samples before the CGE-LIF (Figure 13.) and after the deglycosylation (Figure 14.) to visualize smaller molecular weight of the Fc and Fab fractions without the glycans. Additionally, this implied that the *N*-glycans were indeed released by the PNGaseF activity.

On Figure 14., in lanes 2 and 8, the heavy chain bands are shifted when compared to the same bands in lane 1 and 7, due to the *N*-glycan releasing. The light chain bands in lanes 1-2 and 7-8 are the same size, suggesting a lower level of glycosylation in comparison to the heavy chains. Less prominent band shift is in lane 4 when compared to bands in lane 3. Through the PNGase F activity (upper band), the Fc fragment was deglycosylated. Nevertheless, the faint Fc bands are at two sizes, suggesting an incomplete deglycosylation (the middle band-glycosylated Fc, the lower band-deglycosylated Fc). Probably due to sparely present *N*-glycans on this fraction, the shift is not detected in the Fab bands (lanes 5-6).

Figure 13. The SDS-PAGE separation on the gel of the Fc and Fab fractions from the reduced undigested IgG and digested IgG by the SpeB protease (1 U/µg IgG) on the Fc beads before the deglycosylation (20 hours incubation at 37°C; 1% 2-mercaptoethanol). 1 – Fab fraction of IgG (reduced with 1% 2-mercaptoethanol) without SpeB; 2 – Fc fraction of IgG (reduced with 1% 2-mercaptoethanol) without SpeB; 3 - Fab fraction of digested IgG with SpeB (reduced with 1% 2-mercaptoethanol); 4 – Fc fraction of digested IgG with SpeB (reduced with 1% 2-mercaptoethanol); 5 - IgG (4°C, reduced with 5% 2-mercaptoethanol); 6 – loading dye

* 2-mercaptoethanol was additionally added to all the Fc and Fab samples before loading on the gel to have the final concentration of 5% of the reducing agent
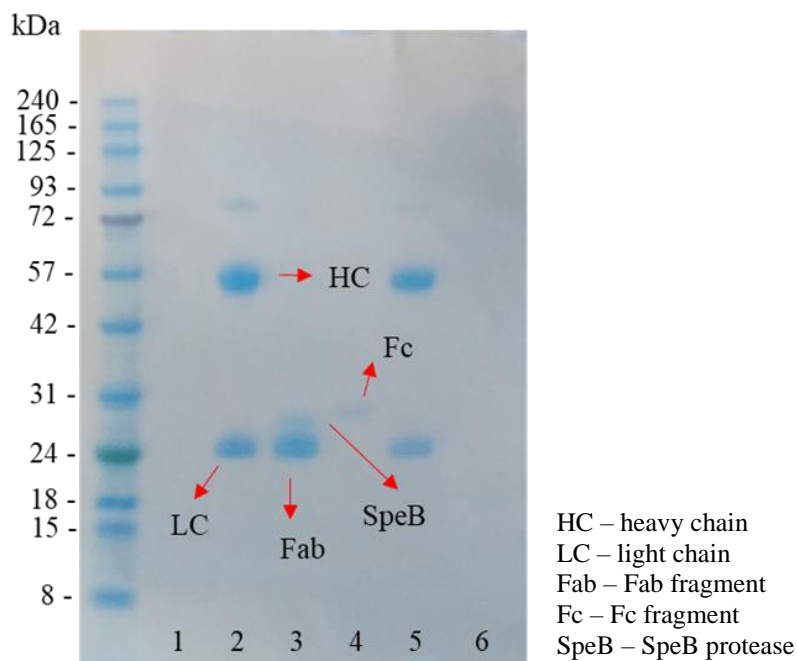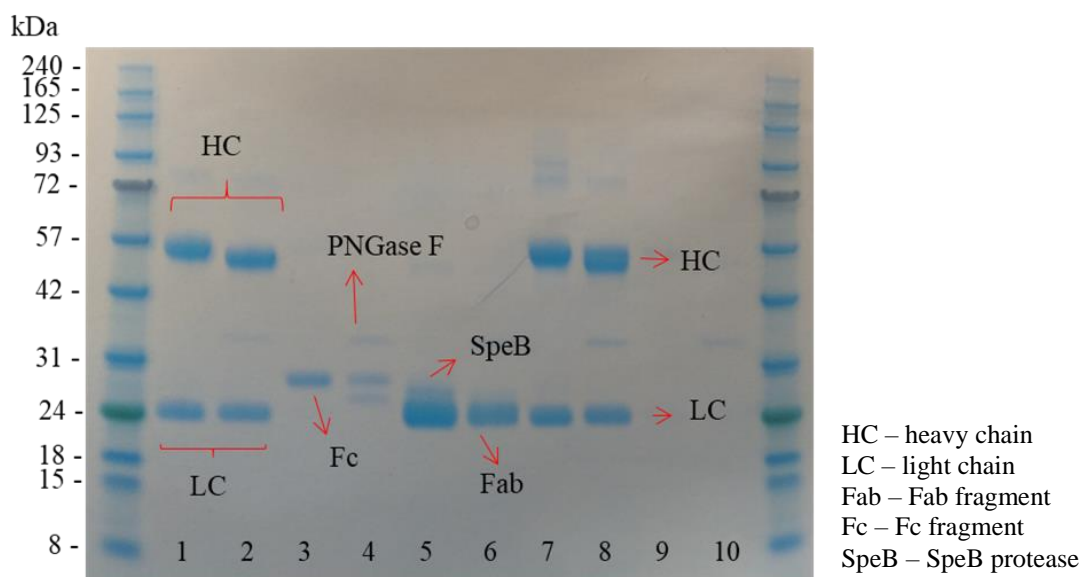
Figure 14. The SDS-PAGE separation on the gel of the Fc and Fab fractions from the reduced undigested IgG and digested IgG by the SpeB protease (1 U/µg IgG) on the Fc beads before and after the deglycosylation (20 hours incubation at 37°C; 1% 2-mercaptoethanol); 1 – IgG 4°C non treated; 2 – IgG 4°C deglycosylated by PNGase F; 3 – Fc (following IgG digestion by SpeB); 4 – Fc (following IgG digestion by SpeB) deglycosylated by PNGase F; 5 – Fab (following IgG digestion by SpeB); 6 – Fab (following IgG digestion by SpeB) deglycosylated by PNGase F; 7- Fc fraction of non-digested IgG; 8 - Fc fraction of non-digested IgG deglycosylated by PNGase F; 9 - Fab fraction of non-digested IgG; 10 – Fab fraction of non-digested IgG + PNGase F

* 2-mercaptoethanol was additionally added to all the Fc and Fab samples before loading on the gel to have the final concentration of 5% of the reducing agent

4.5. CGE-LIF analysis of *N*-glycosylation of mouse Fc and Fab confirms a glycopattern similar to human IgG

After APTS-labelled *N*-glycans were analyzed by CGE-LIF, the obtained data were processed numerically and graphically in the Empower program. The proportion height percentage was used to quantify the abundance of glycan peaks. A total of 35 *N*-glycan peaks were described on the IgG electropherogram at a different normalized migration time units (MTU'') and relative fluorescence units (RFU) values (Figure 15. and Figure 16.). On the electropherogram of control samples (IgG 4°C and 37°C) and the Fc fraction of the undigested IgG, a total of 16 glycan peaks was annotated according to published information (Schaffert *et al.*, 2020).

The control samples show a similar glycan pattern regardless of the incubation temperature. Also, the undigested IgG (Fc fraction) shows values similar to the control samples because total IgG was bound to the Fc beads, eluted without the enzyme activity releasing labelled *N*-glycans which were later analyzed (Figure 15, Table 11). On the contrary, the samples of the Fc and Fab fraction show more differences (Figure 16, Table 11). A more precise distinction between the Fc and Fab glycan peaks can be observed when the percentage of total peak height proportion is taken into consideration (Table 11). The obtained PHP (%) data of the analyzed *N*-glycans from controls and the Fc and Fab fractions is shown in Figure 12. and Figure 13. The PHP (%) of glycan peaks on the Fc fraction shows significantly represented glycan peaks 8, 9, 12, 15, 20, and 21. On the Fab fraction, predominantly observed glycan peaks are 3, 12, 14, 15, and 20. Some peaks show low PHP (%) values in all sample types (peaks 7, 13, 18, 22, 24, 25, 26, and 28) and some were only observed on the Fab fraction (peaks 32-35).

All already known *N*-glycans and their peaks were noted in the control IgG samples. New 19 peaks were also noted, but their identity is not defined. In spite of that, PHP (%) values and observed peaks on the electropherograms were defined for all potential IgG glycan structures. Conclusively, the Fab fraction bears mostly highly processed and sialylated *N*-glycans, while a bigger proportion of neutral (a-, mono- and digalactosylated) *N*-glycans is present on the Fc fraction.

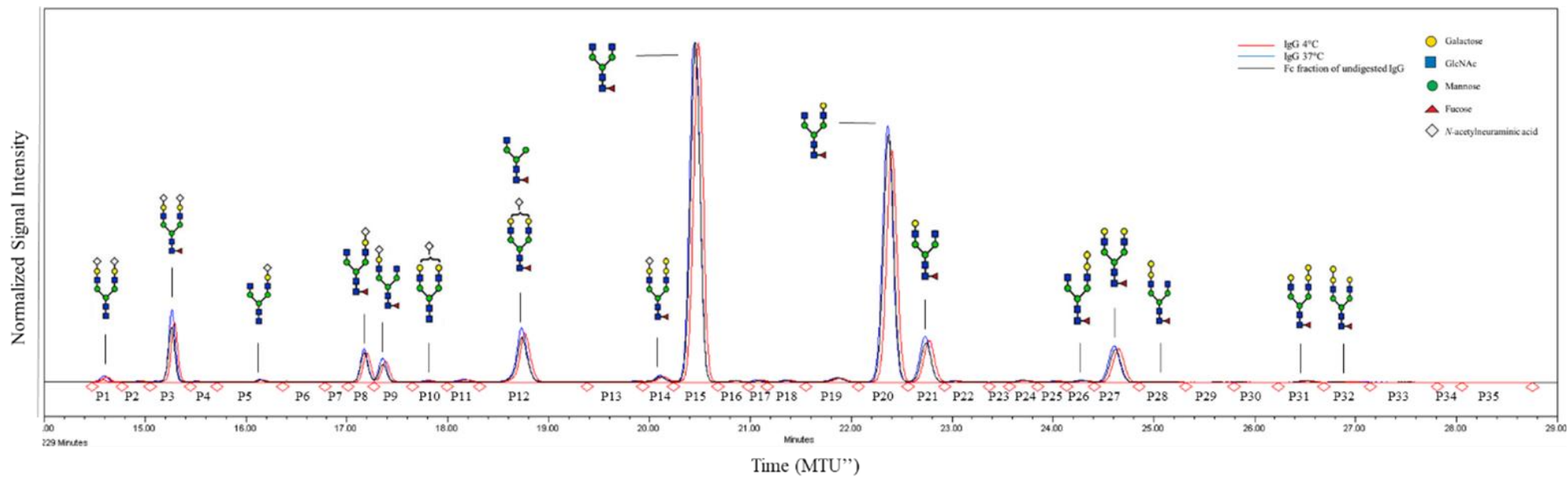*Figure 15.* Electropherogram of analyzed glycans (control samples) with attached known glycan structres.

IgG 4°C – red electropherogram line

IgG 37°C – blue electropherogram line

Fc fraction of undigested IgG - black electropherogram line
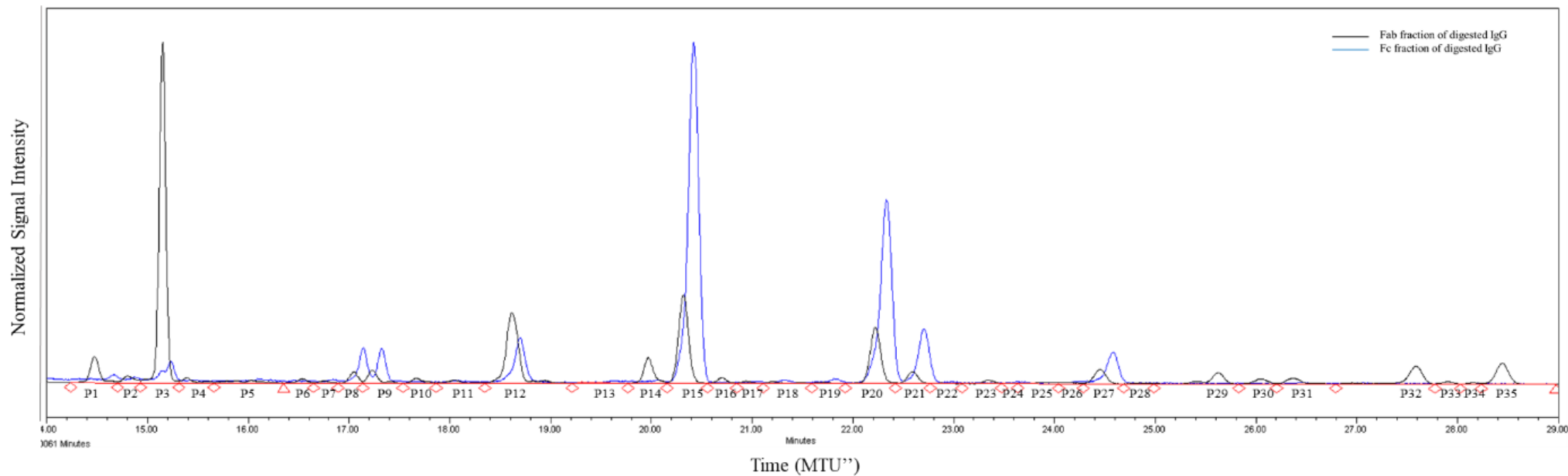
Figure 16. Electropherogram of analyzed glycans (Fc and Fab fractions of digested IgG)

Fab fraction - black electropherogram line

Fc fraction - blue electropherogram line

P - glycan peak

Table 11. Total % PHP (peak height proportion) for each glycan peak (GP) in analysed samples.

Sample	GP1	GP2	GP3	GP4	GP5	GP6
IgG_4°C	0,60	0,11	7,10	0,11	0,27	0,06
IgG_37°C	0,66	0,11	7,91	0,12	0,29	0,08
IgG_undigested_Fc fraction	0,29	0,05	6,53	0,10	0,26	0,11
Fc fraction_10 s_injection	0,67	0,43	2,67	0,17	0,33	0,20
Fab fraction_10 s_injection	3,36	0,89	44,12	0,69	0,36	0,56

Sample	GP7	GP8	GP9	GP10	GP11	GP12
IgG_4°C	0,05	3,43	2,44	0,21	0,30	5,77
IgG_37°C	0,04	3,66	2,62	0,20	0,31	5,97
IgG_undigested_Fc fraction	0,04	3,50	2,09	0,06	0,06	5,34
Fc fraction_10 s_injection	0,33	4,29	4,27	0,13	0,26	5,54
Fab fraction_10 s_injection	0,31	1,49	1,68	0,67	0,42	9,14

Sample	GP13	GP14	GP15	GP16	GP17	GP18
IgG_4°C	0,13	0,68	40,15	0,16	0,26	0,23
IgG_37°C	0,14	0,74	37,41	0,18	0,26	0,23
IgG_undigested_Fc fraction	0,11	0,66	40,53	0,18	0,13	0,16
Fc fraction_10 s_injection	0,13	0,41	42,51	0,21	0,38	0,21
Fab fraction_10 s_injection	0,17	3,32	11,46	0,73	0,30	0,24

Sample	GP19	GP20	GP21	GP22	GP23	GP24
IgG_4°C	0,49	27,41	4,91	0,14	0,06	0,21
IgG_37°C	0,51	28,22	5,06	0,14	0,06	0,24
IgG_undigested_Fc fraction	0,53	29,55	4,67	0,14	0,05	0,24
Fc fraction_10 s_injection	0,54	23,32	6,91	0,23	0,09	0,22
Fab fraction_10 s_injection	0,19	7,28	1,50	0,10	0,48	0,08

Sample	GP25	GP26	GP27	GP28	GP29	GP30
IgG_4°C	0,13	0,20	3,96	0,05	0,03	0,04
IgG_37°C	0,14	0,23	4,02	0,05	0,03	0,04
IgG_undigested_Fc fraction	0,09	0,21	3,96	0,05	0,03	0,04
Fc fraction_10 s_injection	0,17	0,34	4,03	0,14	0,14	0,16
Fab fraction_10 s_injection	0,17	0,14	1,83	0,11	1,45	0,59

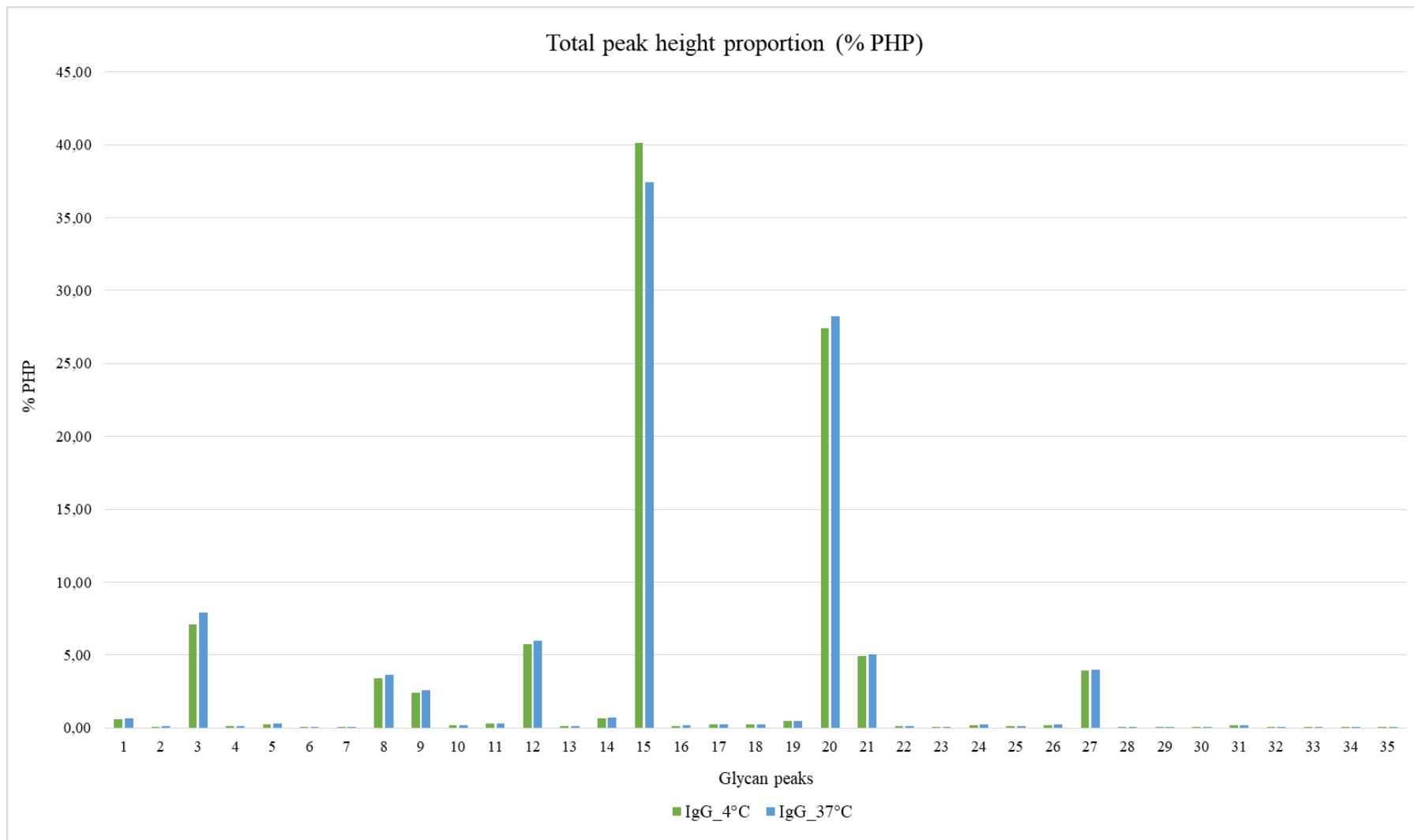| Sample	GP31	GP32	GP33	GP34	GP35
IgG_4°C	0,17	0,05	0,04	0,03	0,03
IgG_37°C	0,17	0,06	0,05	0,03	0,03
IgG_undigested_Fc fraction	0,16	0,04	0,03	0,01	0,02
Fc fraction_10 s_injection	0,20	0,08	0,08	0,09	0,10
Fab fraction_10 s_injection	0,73	2,29	0,27	0,17	2,70

Figure 67. Total peak height proportion (%) for glycan peaks compared in control samples.

Green column – IgG 4°C
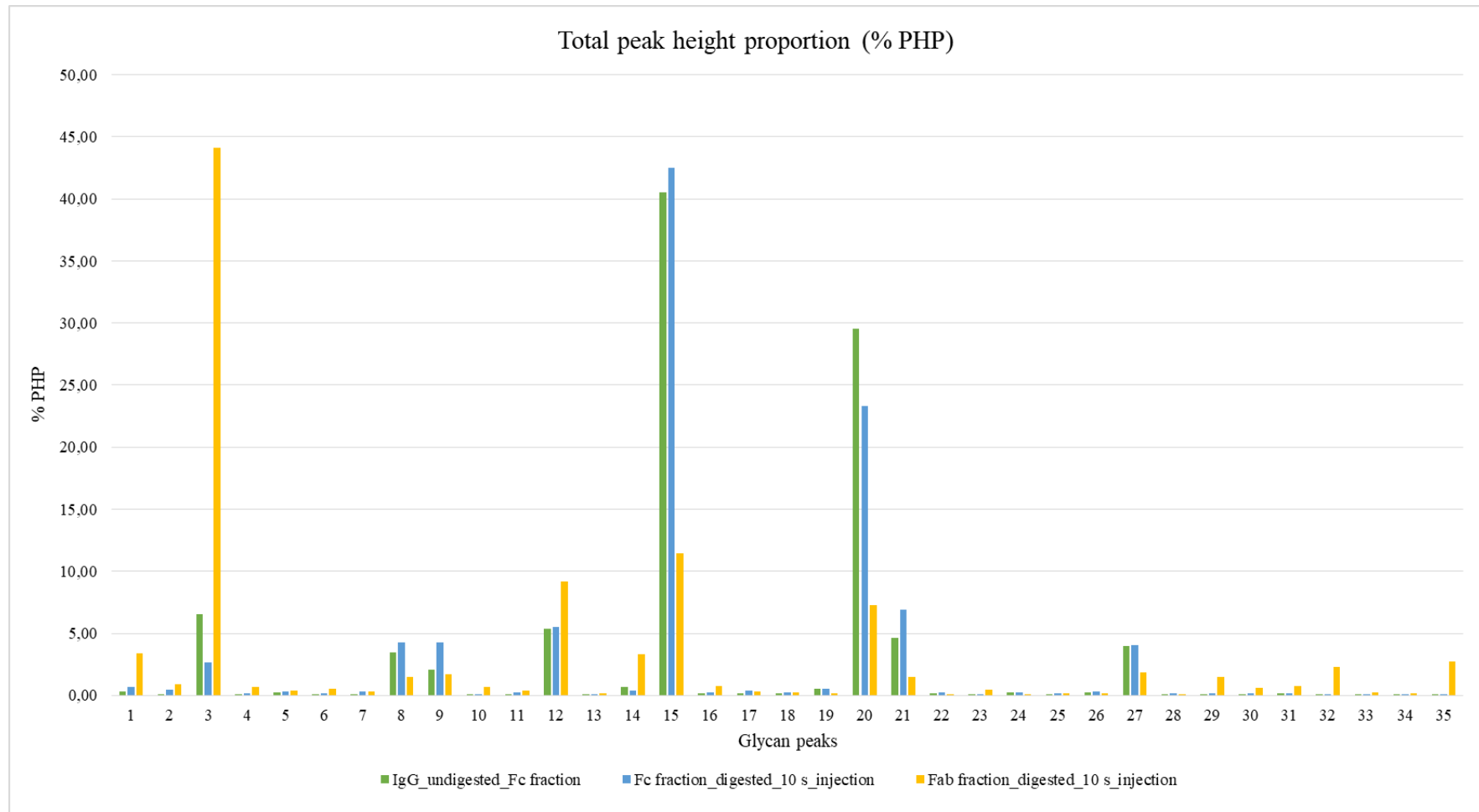
Blue column - IgG 37°C

Figure 18. Total peak height proportion (%) for glycan peaks compared in Fc and Fab samples.

Green – IgG undigested (Fc fraction)

Blue column – Fc fraction

Yellow column – Fab fraction

5. Discussion

Protein *N*-glycosylation is one of the most significant post-translational modifications, directly influencing protein conformation, stability and, in the case of IgG, function. IgG glycosylation has been broadly researched, and the *N*-glycosylation of its Fc fraction is an important feature modulating IgG effector functions. In comparison to thoroughly analyzed Fc *N*-glycans, Fab glycosylation is less explored, although it has recently been implied in the pathogenesis of various diseases. In particular, the comprehensive assessment of the suitability of mice as a model animal in this regard is still lacking. To tackle this question, the method for a separate glycoanalysis of the mouse Fab and Fc fragments needs to be developed. The presented experimental results show that initial conditions for a successful mouse IgG digestion, Fab and Fc separation, and fragment deglycosylation have been established. This allowed for the analysis of the *N*-glycans, originating from the mouse Fab and Fc fractions, with some room for improvement. The initial analysis of the mouse IgG showed differences in the Fab and Fc glycoprofile similar to those observed in the human IgG – namely, the Fab fragment carried more highly processed, sialylated *N*-glycans, while the Fc fragment carried more neutral (a-, mono-, and digalactosylated) *N*-glycans. This difference is thought to arise from a different accessibility of the two regions to the glycosylation machinery in the Golgi compartment (van de Bovenkamp *et al.*, 2016).

To our knowledge, a similar analysis has only been described once in the literature by Mahan and colleagues (2016). Their results and represented methodology were taken into account for the basic experiment design, although some experimental conditions where slightly changed in our study. Our procedures were based on the well-established protocols for human IgG *N*-glycosylation analysis by the CGE-LIF by Hanić *et al.* (2019.), and the current knowledge on mouse Fc and Fab glycosylation.

To isolate IgG from mouse plasma (strain C57/B16), Mahan *et al.* (2016.) used protein A/G columns and 0.1 M citrate buffer in the elution step. The IgG digestion into Fab and Fc fragment was performed in-solution for 1 hour. After the digestion, a 1-hour incubation step was set on the protein A coated magnetic beads in a 96 well PCR plate combined with 96 well magnetic plate to immobilize the beads. Contrary to their approach, in this research (Chapter 3.2. Methods), following an established in-house protocol, Protein G plate was used to isolate the IgG from the mouse serum (distinct strain, CBAT6T6), and 0.1 M formic acid was used to elute the bound IgG. SDS-PAGE confirmed a successful isolation (Figure 6. lane 8). After

testing the SpeB activity in-solution, IgG was applied on the plate containing the Fc beads and was exposed to a 1-hour incubation for binding. The final digestion was then performed on the Fc beads for 20 hours, which seems to have resulted in less incompletely reduced and digested IgG in comparison with the 1-hour digestion (Figure 8. and Figure 10).

Furthermore, different type and volume of beads was used for IgG binding. Contrary to 20 μl of used beads in this experiment, Mahan *et al.* (2016) tested different amounts of protein A beads (1, 5, 10, 15, 20, or 30 μl) to bind and enrich the Fc portions. In this experiment 20 μl of the Fc beads were used but with a moderately higher amount of IgG (25 μg and 100 μg for final digestion before deglycosylation) to get enough Fc and Fab fraction for SDS-PAGE and CGE-LIF. Also, 20 μl of the Fc beads was used for successful separation of the human IgG in previous in-house experiments. Mahan *et al.*, (2016) tested the SpeB protease in two-fold dilutions in the range 0.625-10 U for digestion, which resulted in digestion of > 90 % of the IgG when 10 U/20μg IgG was used. A higher enzyme/IgG (1 U/μg IgG) ratio in this experiment was used based on the producer recommendations. SDS-PAGE after digestion confirmed that the digestion step with 1 U/μg IgG was complete, as there are no bands corresponding to potentially undigested IgG in the Fc fraction (Figure 10., lanes 2, 4, 6, 8 and 10; Figure 11., lanes 2, 4 and 6). However, lower amounts of SpeB with suitable amount of IgG can be further tested. The used 2-mercaptoethanol concentrations were also based on the results of the referred article. In addition, this experiment proved that higher concentrations of 2-mercaptoethanol concentrations do not affect the IgG reduction and SpeB activity.

SDS-PAGE of glycosylated versus non-glycosylated samples demonstrated that deglycosylation of the digested Fc fractions showed room for improvement. The presence of glycosylated Fc fractions after the deglycosylation (Figure 14., lane 4), suggests this reaction for the Fc fragment was incomplete. For the Fc fragment, binding to the Fc beads before digestion with SpeB, maybe later decreases deglycosylation efficiency, as the IgG that had not been bound to the Fc beads showed complete deglycosylation (Figure 14., lane 2) and the IgG that had been previously bound to the Fc beads remained glycosylated to a significant extent (Figure 14., lane 8). By increasing the PNGase F concentration, prolonging incubation time for deglycosylation, or testing other various experimental conditions, this step could be optimized. In the case of Fab, 15-25% of the Fab fragments is glycosylated in humans (van de Bovenkamp *et al.*, 2016). Similar is expected for mouse Fab. Therefore, a lack of gel shift after the Fab deglycosylation could be related to an insufficient amount of the glycosylated Fab fragment to be visible on the gel after cleaving the *N*-glycans, rather than the incomplete deglycosylation. Also, the deglycosylation reaction was tested in duplicates for the Fab and Fc samples but

should be repeated on more samples with wider range of various conditions, including the ones used in this experiment, to get results which could point out to the specific step that disables complete deglycosylation. However, the most prominent *N*-glycan peaks were observed and annotated. More sialylated glycoforms, which are characteristic for the Fab fraction, were the first ones eluted in this experiment and are indeed more abundant on the Fab fragment. The PHP (%) values of annotated glycans (Table 12.) show a higher abundance of neutral glycoforms mostly present on the Fc. These results correspond to the findings Mahan *et al.*, (2016.) acquired from the CGE-LIF analysis as well. However, the glycosylation of murine IgG Fab fraction should be further researched. Considering that the *N*-glycosylation sites near the CDRs make the defining of Fab glycoprofile through glycopeptide analysis impossible for polyclonal IgG, (van de Bovenkamp *et al.*, 2018) CGE-LIF and other methods of analysing released glycans will probably be the methods of choice.

Testing and optimization of all performed reaction steps on a large number and heterogeneous groups of mouse IgG samples (strain, gender, age) is necessary to establish a robust method which gives reproducible results. The initial method described here will enable these more comprehensive studies on mice Fab glycosylation.

Differences between certain strains based on the Fc and the total IgG glycosylation analysis imply that the IgG glycome in mice is under a strong genetic influence in specific-pathogen-free conditions, where no environmental differences exist (Krištić *et al.*, 2018). It would be interesting to research to what extent genetic information could influence in particular Fab *N*-glycoprofile in mice.

Currently, mice are considered to be a good model for human IgG *N*-glycosylation. In spite of some structural differences, the majority of the Fc *N*-glycan features are confirmed to be shared between mice and humans. Due to lack of data, however, mouse Fab glycosylation has not been thoroughly assessed in this aspect and is usually only assumed to correspond to its human counterpart. A comprehensive analysis of mouse Fab glycosylation and its variability in different mouse strains and in different physiological conditions (age, sex) would enable a better understanding of this phenomenon and its role in (pato)physiological processes, as well as a targeted choice of animals in mouse studies modelling human Fab *N*-glycosylation.

6. Conclusions

- An initial method for analyzing Fc and Fab *N*-glycosylation of mouse IgG has been established.

- Fc glycoprofile shows more similarities with total IgG glycoprofile containing mostly neutral (a-, mono-, and digalactosylated) *N*-glycans, while Fab contains mostly highly processed (sialylated) *N*-glycans. Glycopattern distinctions of Fab and Fc fragments are similar to ones observed on human IgG.

- The established method needs to be optimized, in particular with regard to deglycosylation efficiency.

- Following further optimization, and validation, this analytical method could in the future be used in mouse studies researching Fab glycosylation.

7. Literature

Bieberich, E. (2014): Synthesis, processing, and function of N-glycans in N-glycoproteins. *Advances in neurobiology*. 9:47–70.
doi: 10.1007/978-1-4939-1154-7_3.

Berg, M. J., Tymozcko, L. J and Stryer, L. (2013). Biokemija. *Školska knjiga.* Zagreb. 11: 303-325.

Bondt, A., Rombouts, Y., Selman, H. J. M., Hensbergen, P. J., Reiding, R. K., Hazes, M. W. and Dolhain, J. E. M. R., Wuhrer, M. (2014): Immunoglobulin G (IgG) Fab glycosylation analysis using a new mass spectrometric high-throughput profiling method reveals pregnancy-associated changes. *Molecular and Cellular Proteomics*. American Society for Biochemistry and Molecular Biology Inc., 13:3029–3039.
doi: 10.1074/mcp.M114.039537.

Bondt, A., Wührer, M., Martijin, T. K., Hazes, M. W. and Dolhain, J. E. M. R. (2016): Fab glycosylation of immunoglobulin G does not associate with improvement of rheumatoid arthritis during pregnancy. *Arthritis Research & Therapy*. 18:274.
doi: 10.1186/s13075-016-1172-1.

van de Bovenkamp, F. S., Hafkenscheid L., Rispens, T. and Rombouts, Y. (2016): The Emerging Importance of IgG Fab Glycosylation in Immunity. *The Journal of Immunology*. The American Association of Immunologists, 196(4): 1435–1441.
doi: 10.4049/jimmunol.1502136.

van de Bovenkamp, F. S., Derksen, I. L. N., van Breemen, J. M., de Taeye S. W., Oooijewaar-de Heer, P., Sanders, R. W. and Rispens T. (2018): Variable domain N-linked glycans acquired during antigen-specific immune responses can contribute to immunoglobulin G antibody stability. *Frontiers in Immunology*. Frontiers Media S.A., 9(APR).
doi: 10.3389/fimmu.2018.00740.

van De Bovenkamp, F. S., Derksen, I. L. N., Oooijewaar-de Heer, P., van Schie, A. K., Kruithof, S., Berkowska, M. A., van der Schoot, C. E., Ijspeert, H., van der Burg, M., Gils, A., Hafkenscheid, L., Toes, R. E. M., Rombouts, Y., Plomp, Y., Wührer, M., van Haam, M. S., Vidarsson, G. and Rispens T. (2018): Adaptive antibody diversification through N-linked glycosylation of the immunoglobulin variable region. *Proceedings of the National Academy of Sciences of the United States of America*. National Academy of Sciences, 115(8): 1901–1906.
doi: 10.1073/pnas.1711720115.

Cooper, G. M. and Hausman, R. E. (2010): Stanica - molekularni pristup. *Medicinska naklada.* Zagreb.

Cobb, B. A. (2019): The history of IgG glycosylation and where we are now. *Glycobiology*. 30(4): 202-213.
doi: 10.1093/glycob/cwz065.

Ferrara, C., Grau, S., Jäger, C., Sondermann, P., Brünker, P., Waldhauer, I., Hennig, M., Ruf, H., Rufer, A. C., Stihle, M., Umaña, P. and Benz, J. (2011): Unique carbohydrate-carbohydrate interactions are required for high affinity binding between FcγRIII and antibodies lacking core fucose. *Proceedings of the National Academy of Sciences of the United States of America* 108(31): 12669-74.
doi: 10.1073/pnas.1108455108/-/DCSupplemental.

Gornik, O. and Lauc, G. (2008): Glycosylation of serum proteins in inflammatory diseases. *Disease Markers*. IOS Press, 267–278.
doi: 10.1155/2008/493289.

Gudelj, I., Lauc, G. and Pezer, M. (2018): Immunoglobulin G glycosylation in aging and diseases. *Cellular Immunology*. Elsevier 333(July): 65–79.
doi: 10.1016/j.cellimm.2018.07.009.

Guhr, T., Bloem, J., Derksen, I. L. N., Wührer, M., Koenderman, H. L. A., Aalberse, R. C. and Rispens, T. (2011): Enrichment of sialylated IgG by lectin fractionation does not enhance the efficacy of immunoglobulin G in a murine model of immune thrombocytopenia. *PLoS ONE*. PLoS One, 6(6).
doi: 10.1371/journal.pone.0021246.

de Haan, N., Reiding, K. R., Krištić, J., Hipgrave-Ederveen, L. A., Lauc, G. and Wührer, M. (2017): The N-glycosylation of mouse immunoglobulin G (IgG)-fragment crystallizable differs between IgG subclasses and Strains. *Frontiers in Immunology*, 8(May): 1–14.
doi: 10.3389/fimmu.2017.00608.

Hafkenscheid, L., Bondt, A., Scherer, U. H., Huizinga, W. J. T., Wührer, M., Toes, E. M. R. and Rombouts, Y. (2017): Structural analysis of variable domain glycosylation of anti-citrullinated protein antibodies in rheumatoid arthritis reveals the presence of highly sialylated glycans. *Molecular and Cellular Proteomics*. American Society for Biochemistry and Molecular Biology Inc., 16(2): 278–287.
doi: 10.1074/mcp.M116.062919.

Karsten, C. M., Pandey, M. K., Figee, J., Kilchenstein, R., Taylor, R. P., Rosas, M., McDonald, U. J., Orr, J. S., Berger, M., Petzold, D., Blanchard, V., Winkler, A., Hess, C., Reid, M. D., Majoul, V. I., Strait, T. R., Harris, L. N., Köhl, G., Wex, E., Ludwig R., Zilikens, D., Nimmerjahn, J., Finkleman D. F., Brown D. G., Ehlers, M. and Köhl, J. (2012): Anti-inflammatory activity of IgG1 mediated by Fc galactosylation and association of FcγRIIB and dectin-1. *Nature Medicine*. Nat Med, 18(9): 1401–1406.
doi: 10.1038/nm.2862.

Käsermann, F., Boerema, J. D., Rüegsegger, M., Hofmann, A., Wymann, S., Zuercher W. A. and Miescher, S. (2012): Analysis and functional consequences of increased fab-sialylation of intravenous immunoglobulin (IVIG) after lectin fractionation. *PLoS ONE*. Public Library of Science, 7(6): 37243.
doi: 10.1371/journal.pone.0037243.

Krištić, J., Zaytseva, O. O., Ram, R., Nguyen, Q., Novokmet, M., Vučković, F., Vilaj, M., Trbojević-Akmačić, I., Pezer, M., Davern, M. K., Morahan, G. and Lauc, G. (2018): Profiling and genetic control of the murine immunoglobulin G glycome. *Nature Chemical Biology*, 14(5): 516–524.
doi: 10.1038/s41589-018-0034-3.

Leibiger, H., Wüstner, D., Stigler, R. D. and Marx U. (1999): Variable domain-linked oligosaccharides of a human monoclonal IgG: structure and influence on antigen binding. *Biochemical Journal*. Portland Press Ltd, 338(Pt 2): 529.
doi: 10.1042/bj3380529.

Liu, H. and May, K. (2012): mAbs Disulfide bond structures of IgG molecules Structural variations, chemical modifications and possible impacts to stability and biological function. *www.landesbioscience.com mAbs*, 4(1): 17–23.
doi: 10.4161/mabs.4.1.18347.

Lu, G., Crihfield, L. C., Gattu, S., Veltri, M. L. and Holland, A. L. (2018): Capillary Electrophoresis Separations of Glycans. *Chemical Reviews*. American Chemical Society, 7867–7885.
doi: 10.1021/acs.chemrev.7b00669.

Lu, L. L., Suscovich, J. T., Fortune, M. S. and Alter G. (2017): Beyond binding : antibody effector. *Nature Reviews Immunology.* Nature Publishing Group, 18: 46–61.
doi: 10.1038/nri.2017.106.

Mahan, A. E., Tedesco, J., Dionne, K., Baruah, K., Cheng, D. H., De Jager, L. P., Barouch, H. D., Susovich, T., Ackerman, M., Crispin M. and Alter G. (2016): A method for high-throughput, sensitive analysis of IgG Fc and Fab glycosylation by capillary electrophoresis. *Journal of Immunological Methods*. (857): 34–44.
doi: 10.1016/j.jim.2014.12.004.A.

Maresch, D. and Altmann, F. (2016): Isotype-specific glycosylation analysis of mouse IgG by LC-MS. *Proteomics*, 1321–1330.
doi: 10.1002/pmic.201500367.

Mestas, J. and Hughes, C. C. W. (2004): Of Mice and Not Men: Differences between Mouse and Human Immunology. *The Journal of Immunology*. The American Association of Immunologists, 172(5): 2731–2738.
doi: 10.4049/jimmunol.172.5.2731.

Michaelsen, T. E., Kolberg, J., Aase, A., Herstad, K. T. and Høiby, A. E. (2004): The four mouse IgG isotypes differ extensively in bactericidal and opsonophagocytic activity when reacting with the P1.16 epitope on the outer membrane PorA protein of Neisseria meningitidis. *Scandinavian Journal of Immunology*. Scand J Immunol, 59(1): 34–39.
doi: 10.1111/j.0300-9475.2004.01362.x.

Reiding, K. R., Hipgrave Ederveen, L. A., Rombouts, Y. and Wührer, M. (2016): Murine Plasma N-Glycosylation Traits Associated with Sex and Strain. *Journal of Proteome Research*. American Chemical Society, 15(10): 3489–3499.
doi: 10.1021/acs.jproteome.6b00071.

Saldova, R., Piccard, H., Perez-Garay, M., Harvey, J. D., Struwe, B. W., Galligan, C. M., Berghmans, N., Madden, F. S., Peracaula, R., Opdenakker, G. and Rudd, M. P. (2013): Increase in Sialylation and Branching in the Mouse Serum N-glycome Correlates with Inflammation and Ovarian Tumour Progression. *PLoS ONE*. 8(8): e71159
doi: 10.1371/journal.pone.0071159.

Schaffert, A., Hanić, M., Novokmet, M., Zaytseva, O. O., Krištić, J., Lux, A., Nitschke, L., Peipp, M., Pezer, M., Hennig, R., Rapp, E., Lauc, G. and Nimmerjahn, F. (2020): Minimal B Cell Extrinsic IgG Glycan Modifications of Pro- and Anti-Inflammatory IgG Preparations in vivo. *Frontiers in Immunology*. Frontiers Media S.A., 10.
doi: 10.3389/fimmu.2019.03024.

Schroeder, H. W. and Cavacini, L. (2010): Structure and function of immunoglobulins. *Journal of Allergy and Clinical Immunology*. Elsevier Ltd, 125(2 SUPPL. 2): S41–S52. doi: 10.1016/j.jaci.2009.09.046.

Sela-Culang, I., Kunik, V. and Ofran, Y. (2013): The structural basis of antibody-antigen recognition. *Frontiers in Immunology*. Frontiers Media SA, 4(OCT). doi: 10.3389/fimmu.2013.00302.

Shields, R. L., Lai, J., Keck, R., O'Connell, Y. L., Hong, K., Meng, G. Y., Weikert, H. A. S. and Presta, G. L. (2002): Lack of fucose on human IgG1 N-linked oligosaccharide improves binding to human FcγRIII and antibody-dependent cellular toxicity. *Journal of Biological Chemistry*. American Society for Biochemistry and Molecular Biology, 277(30): 26733–26740. doi: 10.1074/jbc.M202069200.

Symbol and Text Nomenclature for Representation of Glycan Structure Nomenclature Committee Consortium for Functional Glycomics (2012). http://www.functionalglycomics.org/static/consortium/CFGnomenclature.pdf

Varki, A., Cummings, R. D., Esko, D. J., Stanley, P., Hart, W. G., Aebi, M., Darvill, G. A., Kinoshita, T., Packer, H. N., Prestegard, J. H., Schnaar, R. L. and Seeberger, H. P. (2017): Essentials of Glycobiology. *Cold Spring Harbor Laboratory Press.* Cold Spring Harbor. doi: 10.1101/glycobiology.3e.009

Vidarsson, G., Dekkers, G. and Rispens, T. (2014): IgG subclasses and allotypes: From structure to effector functions. *Frontiers in Immunology*. Frontiers Media S.A., 5(OCT): 520. doi: 10.3389/fimmu.2014.00520.

Wiedeman, A. E., Santer, M. D., Yan, W., Miescher, S., Käsermann and Elkon, B. K. (2013): Contrasting mechanisms of interferon-α inhibition by intravenous immunoglobulin after induction by immune complexes versus toll-like receptor

agonists. *Arthritis and Rheumatism*. Arthritis Rheum, 65(10): 2713–2723.
doi: 10.1002/art.38082.

Zaytseva, O. O., Jansen, C. B., Hanić, M., Mrčela, M., Razdorov, G., Stojković, R., Erhardt, J., Brizić, I., Jonjić, S., Pezer, M. and Lauc, G. (2018): MIgGGly (mouse IgG glycosylation analysis) - a high-throughput method for studying Fc-linked IgG N-glycosylation in mice with nanoUPLC-ESI-MS. *Scientific Reports*. Nature Publishing Group, 8(1).
doi: 10.1038/s41598-018-31844-1.

Zhu, Z., Lu, J. J. and Liu, S. (2012): Protein separation by capillary gel electrophoresis: A review. *Analytica Chimica Acta*. NIH Public Access, 21–31.
doi: 10.1016/j.aca.2011.10.022.

Web 1 - http://www.brainkart.com/article/Structure-of-Immunoglobulins_17908/
(accessed 25.10.2020.)

Web 2 - https://www.genovis.com/products/igg-proteases/fabulous/fabulous-enzyme/
(accessed 4.1.2021.)

8. Appendix

8.1. Approval by Croatian Ministry of Agriculture for using animal models in experiment

9. Curriculum vitae

I was born in Varaždin, 18.12.1995. I graduated from highschool Prva Gimnazija Varaždin and then started undergraduate study programe of Biology in 2015. at Department of Biology, Josip Juraj Strossmayer University of Osijek. During undergraduate study programme I was working as Student Demonstrator through laboratory practices as a part of the Anatomy and Histology subject. Also I was included in organization of the science popularization projects (*„Biolog i ja“, „Brain Awareness Week“, „Science Festival“).* In 2018. I finished undergraduate study programme and started graduate study program of Experimental Biology (Physiology and Immunobiology) at Department of Biology, Faculty of Science in Zagreb. During graduate study programme in 2019. I was working through students practice in Genos Glycoscience Ltd., and was part of the organization team for two events - *„WISe - WorkIn Science 2019.“* and *„Meet the Biologists 2020“.* Together with my collegues, in 2020. I got Rector's Award for organization of *„Meet the Biologists 2020. – HRZZ edition“.* During 2020. I performed experimental part of my master thesis in Genos Glycoscience Ltd. and in November 2020. attended Virtual Annual Meeting (''*Uncharted Waters''*) of *Society for Glycobiology* where I presented results of my master thesis experiment in poster form. In November 2020. I started working as Junior Scientist – Bioanalyst in Drug Metabolism and Pharmacokinetics Department (DMPK) at Fidelta Ltd. in Zagreb.